THEORY

Adaptive Backstepping Control Based on Global HOSM Differentiators With Dynamic Gains

MARCELO LUIZ DE CARVALHO MOURA MOREIRA[1],
TIAGO ROUX OLIVEIRA[2], (Senior Member, IEEE),
AND KURIOS IURI PINHEIRO DE MELO QUEIROZ[3]

[1]Department of Transmission Expansion Studies, Energy Research Office (EPE), Rio de Janeiro 20091-040, Brazil
[2]Department of Electronics and Telecommunication Engineering, State University of Rio de Janeiro (UERJ), Rio de Janeiro 20550-011, Brazil
[3]Department of Electrical Engineering, Federal University of Rio Grande do Norte (UFRN), Natal 59078-970, Brazil

Corresponding author: Marcelo Luiz de Carvalho Moura Moreira (moreiramarceloluiz@gmail.com)

ABSTRACT The present paper proposes the application of global and exact differentiators with dynamic gains based on higher-order sliding modes (*HOSM*) to the design of adaptive *backstepping* control for nonlinear uncertain systems of *strict-feedback* type. The use of this kind of differentiator in the closed-loop system allow us to guarantee global uniform stability (for any initial conditions) due to the variable nature of the dynamic gain. The dynamic gain can grow or decrease with the unmeasured state. In addition, asymptotic output tracking is also assured. In order to illustrate the results of the new theorem, the proposed controller is applied to a high-performance aircraft system, suppressing the wing-rock phenomenon usually observed for fast-speed flight conditions. Comparison results with a linear-inexact differentiator, a local *HOSM* differentiator with fixed gains and the proposed global and exact *HOSM* differentiator with dynamic gain shows the superiority of the latter over the former approaches. To demonstrate the practical efficacy of the proposed approach, we conclude with an experimental test featuring a DC motor and the novel differentiator-based backstepping control scheme.

INDEX TERMS Adaptive systems, backstepping control, global sliding mode differentiator, uncertain nonlinear systems.

I. INTRODUCTION

Basically, the theory of nonlinear control can be roughly divided into robust and adaptive methods. In adaptive systems the control law is designed using dynamic estimates for the unknown parameters of the plant. In this way, gains are adjusted all the time from a given adaptation law. In robust control, in general, we try to guarantee stability properties with fixed (or even dynamic) gains for a given range of variation of the plant parameters, which is the case, for example, of the sliding mode control [1].

A. LITERATURE REVIEW

In this sense, the backstepping control [2], [3] allows certain state variables to act as "virtual control inputs" of other variables, forming a cascade control project. This technique is restricted to a certain class of systems called *strict-feedback*

which name is given by the presence of a recursion in the state equations that are dependent on each other (the nonlinearities in the $\dot{x}_i$–equation depends only on the state variables $x_1, x_2, \ldots, x_i$). In other words, all the unknown information is lumped into the last state equation [4], [5]. This control strategy has several applications, for example, in electric motors [6], diesel machines [7], jet engines [8], robotics [9], quadcopters [10], ship positioning [11], control of air vehicles [12] and attitude control of spacecrafts [13].

With the work of Krstić et al. [14], it was possible to attenuate the degree of complexity of the original backstepping controller since the number of parameters to be adapted became small with the introduction of tuning functions. Despite this effort, the task of analyzing and designing such controllers remains arduous.

New methods are presented in [15] and [16] to enable the use of the adaptive backstepping approach in applications that were prohibitively difficult by the conventional method with analytic derivatives, ending the complexity arising due

to the "explosion of terms" that has made other techniques difficult to implement in practice. Futhermore, reference [17] mitigates the control design using the backstepping procedure by combining the feedback linearization technique with the high-order sliding modes. However it's application was only valid to linear systems and also using fixed gain.

In [18], with the help of local exact differentiators based on higher-order sliding modes and fixed gains [19], a new perspective for adaptive backstepping control has emerged. The proposal of [18] dramatically simplifies the control design since it extinguishes the calculation of partial derivatives of the stabilization functions required in the backstepping by tuning functions [14]. However, this work did not present the proof of stability for the class of nonlinear systems considered (of the *strict-feedback* type) and, with that, it gave us the opportunity to advance in this topic in order to obtain a rigorous stability proof not presented in the literature yet.

B. RESULTS AND CONTRIBUTIONS

The main ingredient proposed for this generalization was the introduction of an exact differentiator based on higher-order sliding modes (HOSM) with dynamic gains [20] in order to guarantee the global stability of the modified backstepping controller. This result is innovative since with the fixed-gains a differentiator in [17] and [18], only local results could be achieved or a very restricted class of systems could be considered.

The use of the HOSM Differentiator with Dynamic Gains and finite time convergence allows for a much simpler control design while preserves the global stability and output tracking properties of the closed-loop system. Note that if we simply employ standard exact HOSM differentiator with fixed gains, we would lose the globality and only local stability results could be proved.

Another possibility to replace the global HOSM differentiator is to use the more involved Kreisselmeier filters [21], similar to linear differentiators, as done in traditional backstepping control. However, as a rule of thumb: the simpler adaptation law, the better is the transient performance since the convergence rate of the adaptation law is directly related to the amount of filters applied to derive it as well as the type of convergence achieved. Each filter imposes an additional layer of adaptation with its own demanding dynamics to settle down. In the traditional and more involved backstepping designs, none of such filter dynamics converges in finite time, compromising the transient performance of the overall scheme. In addition, the proposed adaptive backstepping approach based on dynamic gains is still simpler than more recent backstepping control versions including neural networks components [22] and/or sliding mode architectures for the filter designs [23].

C. ORGANIZATION

- The second section is dedicated to briefly revisiting the theory of traditional backstepping control [24].

- The third section presents the problem formulation, showing the type of plant to be studied (*in the strict-feedback form*) and the backstepping adaptive control approach through tuning functions [18].
- The fourth section describes the proposed HOSM exact differentiator with dynamic gains which will be employed in the proposed recipe for the new adaptive backstepping control of the next section.
- The fifth section also states the main theorem with the proof of global stability for the closed-loop system.
- The sixth section presents the simulation results involving the proposed controller via global HOSM differentiator and dynamic gains by comparing its performance with two other differentiation schemes: a linear differentiator and another HOSM differentiator with fixed gain. An engineering application example considering the Wing Rock control problem is considered for the evaluation scenario.
- The seventh section brings preliminary experimental tests with a DC motor to illustrate the potential of the proposed approach in a real-world scenario.
- The eighth section concludes the paper highlighting the obtained advances according to our initial objectives and discusses about future directions of investigation.

II. REVISITING THE TRADITIONAL BACKSTEPPING ADAPTIVE CONTROL

The backstepping control procedure involves recursively selecting appropriate state variable stabilization functions to act as inputs for a pseudo-control (virtual control laws) of smaller subsystems, obtained during the control design for the entire system. Each adaptive control stage produces a new pseudo-control input for each subsystem, which is again expressed in terms of the pseudo-control signal previously obtained. This process is repeated until the actual control law is obtained in the final stage.

For this reason, adaptive backstepping control is a systematic iterative control design method. It is based on state feedback with a final control law given by a *Lyapunov* control function (*LCF*) and the dynamics of the closed-loop system.

First of all, we will consider a nonlinear system of the *strict-feedback* type according to Figure 1 and described below [24]:

$$\dot{x}_1 = x_2 + \theta^{*T}\varphi_1(x_1)$$
$$\dot{x}_2 = x_3 + \theta^{*T}\varphi_2(x_1, x_2)$$
$$\vdots$$
$$\dot{x}_{n-1} = x_n + \theta^{*T}\varphi_{n-1}(x_1, \ldots, x_{n-1})$$
$$\dot{x}_n = \beta u + \theta^{*T}\varphi_n(x)$$
$$y = x_1. \tag{1}$$

The vector $x = [x_1, \ldots, x_n] \in \mathbb{R}^n$, $u \in \mathbb{R}$ and $y \in \mathbb{R}$ are the state vector, the input and output signals of the system, respectively. The vector of unknown constants θ^* need to be estimated throughout the design of the adaptation law. The
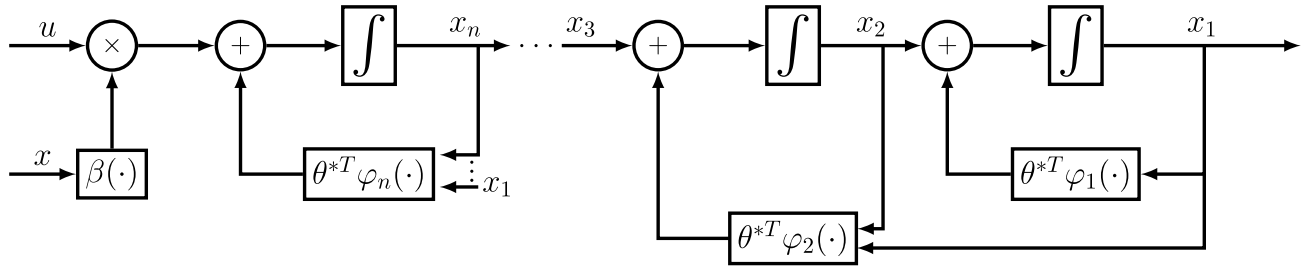
FIGURE 1. Nonlinear system in the *strict-feedback* type with order *n*.

vector that has known nonlinear functions is given by $\varphi_i \in \mathbb{R}$ for $i = 1, \ldots, n$. The term $\beta \neq 0$ is a known constant. In this system, nonlinearities depend purely on the variables being fed back.

The control objective is to force the output $y(t)$ to track the reference signal $y_r(t)$, while keeping all the closed-loop signals uniformly bounded. The controller is developed using an iterative procedure as shown below.

A. DEFINITION OF ERROR VARIABLES z_1 AND z_2

Consider

$$z_1 = x_1 - y_r, \tag{2}$$

$$z_2 = x_2 - \dot{y}_r - \alpha_1, \tag{3}$$

where z_1 is the output tracking error and it is intended to ensure that it will ultimately converge to zero, that is, $\lim_{t \to \infty} z_1(t) = 0$. Thus, the time derivative of z_1 is defined as

$$\dot{z}_1 = \dot{y} - \dot{y}_r,$$
$$= x_2 + \theta^{*T} \varphi_1 - \dot{y}_r,$$
$$= z_2 + \alpha_1 + \theta^{*T} \varphi_1, \tag{4}$$

where α_1 it is the first virtual control input to stabilize the output tracking error z_1. It is defined as

$$\alpha_1 = -c_1 z_1 - \hat{\theta}^T \varphi_1. \tag{5}$$

Here, the constant c_1 is positive and $\hat{\theta}(t)$ is the estimate of θ^*. The first virtual control entry α_1 acts as the desired value of x_2 in order to make the z_1-subsystem stable.

The first *Lyapunov* function is defined as

$$V_1 = \frac{1}{2} z_1^2 + \frac{1}{2} \tilde{\theta}^T \Gamma^{-1} \tilde{\theta}, \tag{6}$$

where Γ is a positive-definite matrix and $\tilde{\theta}$ is the estimation error, defined by $\tilde{\theta} = \theta^* - \hat{\theta}$. Through equations (4) and (5), the first-time derivative of V_1 is calculated as

$$\dot{V}_1 = z_1 \left(-c_1 z_1 + z_2 + \tilde{\theta}^T \varphi_1 \right) - \tilde{\theta}^T \Gamma^{-1} \dot{\hat{\theta}}$$
$$= z_1 (-c_1 z_1 + z_2) - \tilde{\theta}^T \left(\Gamma^{-1} \dot{\hat{\theta}} - \varphi_1 z_1 \right). \tag{7}$$

The tuning function is defined as

$$\tau_1 = \varphi_1 z_1. \tag{8}$$

Replacing (8) into (7), results in

$$\dot{V}_1 = -c_1 z_1^2 + z_1 z_2 - \tilde{\theta}^T \left(\Gamma^{-1} \dot{\hat{\theta}} - \tau_1 \right). \tag{9}$$

In order to guarantee $\dot{V}_1 \leq 0$, the term $z_1 z_2$ needs to be canceled.

B. DEFINITION OF THE ERROR VARIABLE z_3

Now, the next error variable z_3 will be defined and then the subsystem (z_1, z_2) is studied:

$$z_3 = x_3 - \ddot{y}_r - \alpha_2. \tag{10}$$

From (3) and using (5), taking the derivative of z_2 we arrive at

$$\dot{z}_2 = \dot{x}_2 - \ddot{y}_r - \alpha_2$$
$$= z_3 + \alpha_2 - \frac{\partial \alpha_1}{\partial x_1} x_2 + \theta^{*T} \left(\varphi_2 - \frac{\partial \alpha_1}{\partial x_1} \varphi_1 \right) +$$
$$- \frac{\partial \alpha_1}{\partial y_r} \dot{y}_r - \frac{\partial \alpha_1}{\partial \hat{\theta}} \dot{\hat{\theta}}, \tag{11}$$

where α_2 is the second virtual control input to stabilize the system (z_1, z_2) in (4) and (11):

$$\alpha_2 = -z_1 - c_2 z_2 + \frac{\partial \alpha_1}{\partial x_1} x_2 - \hat{\theta}^T \left(\varphi_2 - \frac{\partial \alpha_1}{\partial x_1} \varphi_1 \right) +$$
$$+ \frac{\partial \alpha_1}{\partial y_r} \dot{y}_r + \frac{\partial \alpha_1}{\partial \hat{\theta}} \Gamma \tau_2. \tag{12}$$

Equation (12) guarantees the stability of the subsystem (4) and (11). In (12), we have c_2 as a positive constant and the second tuning function τ_2 based on τ_1 as follows

$$\tau_2 = \tau_1 + \left(\varphi_2 - \frac{\partial \alpha_1}{\partial x_1} \varphi_1 \right) z_2. \tag{13}$$

The conditions for the proof stability of the subsystem (z_1, z_2) requires a second *Lyapunov* candidate function that is chosen by

$$V_2 = V_1 + \frac{1}{2} z_2^2. \tag{14}$$

From equations (9), (11)-(13), the time derivative of V_2 can be calculated as

$$\dot{V}_2 = -c_1 z_1^2 + z_1 z_2 - \tilde{\theta}^T \left(\Gamma^{-1} \dot{\hat{\theta}} - \tau_1 \right) + z_2(-z_1 - c_2 z_2 +$$

$$+ z_3) + z_2 \hat{\theta}^T \left(\varphi_2 - \frac{\partial \alpha_1}{\partial x_1} \varphi_1 \right) + z_2 \frac{\partial \alpha_1}{\partial \hat{\theta}} \left(\Gamma \tau_2 - \dot{\hat{\theta}} \right) ,$$

$$\dot{V}_2 = -c_1 z_1^2 - c_2 z_2^2 + z_2 z_3 + \tilde{\theta}^T \left(\tau_2 - \Gamma^{-1} \dot{\hat{\theta}} \right) +$$

$$+ z_2 \frac{\partial \alpha_1}{\partial \hat{\theta}} \left(\Gamma \tau_2 - \dot{\hat{\theta}} \right) . \tag{15}$$

C. DEFINITION OF THE ERROR VARIABLE z_4

Analogous to the previous steps, we define

$$z_4 = x_4 - \dddot{y}_r - \alpha_3 . \tag{16}$$

Now, the subsystem is (z_1, z_2, z_3) and to deal with this, we use the dynamic error z_3 which is found from the derivative of (11) along of (1), (13), (16), such that

$$\dot{z}_3 = z_4 + \alpha_3 - \frac{\partial \alpha_2}{\partial x_1} x_2 - \frac{\partial \alpha_2}{\partial x_2} x_3 + \theta^{*T} (\varphi_3 - \frac{\partial \alpha_2}{\partial x_1} \varphi_1 +$$

$$- \frac{\partial \alpha_2}{\partial x_2} \varphi_2) - \frac{\partial \alpha_2}{\partial y_r} \dot{y}_r - \frac{\partial \alpha_2}{\partial \dot{y}_r} \ddot{y}_r - \frac{\partial \alpha_2}{\partial \hat{\theta}} \dot{\hat{\theta}} . \tag{17}$$

The third virtual control input is α_3:

$$\alpha_3 = -z_2 - c_3 z_3 + \frac{\partial \alpha_2}{\partial x_1} x_2 + \frac{\partial \alpha_2}{\partial x_2} x_3 - \hat{\theta}^T \left(\varphi_3 - \frac{\partial \alpha_2}{\partial x_1} \varphi_1 + \right.$$

$$\left. - \frac{\partial \alpha_2}{\partial x_2} \varphi_2 \right) + \frac{\partial \alpha_2}{\partial y_r} \dot{y}_r + \frac{\partial \alpha_2}{\partial \dot{y}_r} \ddot{y}_r + \frac{\partial \alpha_2}{\partial \hat{\theta}} \Gamma \tau_3 +$$

$$+ z_2 \frac{\partial \alpha_1}{\partial \hat{\theta}} \Gamma \left(\varphi_3 - \frac{\partial \alpha_2}{\partial x_1} \varphi_1 - \frac{\partial \alpha_2}{\partial x_2} \varphi_2 \right) , \tag{18}$$

with c_3 being a positive constant and the third tuning function τ_3 based on τ_2 defined by

$$\tau_3 = \tau_2 + \left(\varphi_3 - \frac{\partial \alpha_2}{\partial x_1} \varphi_1 - \frac{\partial \alpha_2}{\partial x_2} \varphi_2 \right) z_3 . \tag{19}$$

Considering the third *Lyapunov* candidate V_3 for the subsystem (z_1, z_2, z_3):

$$V_3 = V_2 + \frac{1}{2} z_3^2 . \tag{20}$$

From (16), (18) and (19), the time derivative of V_3 can be calculated as

$$\dot{V}_3 = -c_1 z_1^2 - c_2 z_2^2 - c_3 z_3^2 + z_3 z_4 + \tilde{\theta}^T \left(\tau_3 - \Gamma^{-1} \dot{\hat{\theta}} \right) +$$

$$+ z_2 \frac{\partial \alpha_1}{\partial \hat{\theta}} \left(\Gamma \tau_2 - \dot{\hat{\theta}} \right) + z_3 \frac{\partial \alpha_2}{\partial \hat{\theta}} \left(\Gamma \varphi_3 - \dot{\hat{\theta}} \right) +$$

$$+ z_2 \frac{\partial \alpha_1}{\partial \hat{\theta}} \Gamma \left(\varphi_3 - \frac{\partial \alpha_2}{\partial x_1} \varphi_1 - \frac{\partial \alpha_2}{\partial x_2} \varphi_2 \right) z_3 . \tag{21}$$

Recalling that,

$$z_2 \frac{\partial \alpha_1}{\partial \hat{\theta}} \left(\Gamma \tau_2 - \dot{\hat{\theta}} \right) = z_2 \frac{\partial \alpha_1}{\partial \hat{\theta}} (\Gamma \tau_3 - \dot{\hat{\theta}}) + z_2 \frac{\partial \alpha_1}{\partial \hat{\theta}} \Gamma (\tau_2 - \tau_3)$$

$$= z_2 \frac{\partial \alpha_1}{\partial \hat{\theta}} (\Gamma \tau_3 - \dot{\hat{\theta}}) - z_2 \frac{\partial \alpha_1}{\partial \hat{\theta}} \Gamma (\varphi_3 +$$

$$- \frac{\partial \alpha_2}{\partial x_1} \varphi_1 - \frac{\partial \alpha_2}{\partial x_2} \varphi_2) z_3 , \tag{22}$$

and replacing (22) into (21), one has

$$\dot{V}_3 = -c_1 z_1^2 - c_2 z_2^2 - c_3 z_3^2 + z_3 z_4 + \tilde{\theta}^T \left(\tau_3 - \Gamma^{-1} \dot{\hat{\theta}} \right) +$$

$$+ \left(z_2 \frac{\partial \alpha_1}{\partial \hat{\theta}} + z_3 \frac{\partial \alpha_2}{\partial \hat{\theta}} \right) \left(\Gamma \tau_3 - \dot{\hat{\theta}} \right) . \tag{23}$$

D. DEFINITION OF THE ERROR VARIABLE z_i

The error z_i and its derivative are defined below:

$$z_i = x_i - y_r^{(i-1)} - \alpha_{i-1} ,$$

$$\dot{z}_i = z_{i+1} + \alpha_i - \sum_{k=1}^{i-1} \frac{\partial \alpha_{i-1}}{\partial x_k} x_{k+1} + \theta^{*T} (\varphi_i +$$

$$- \sum_{k=1}^{i-1} \frac{\partial \alpha_{i-1}}{\partial x_k} \varphi_k) - \sum_{k=1}^{i-1} \frac{\partial \alpha_{i-1}}{\partial y_r^{k-1}} y_r^{(k)} - \frac{\partial \alpha_{i-1}}{\partial \hat{\theta}} \dot{\hat{\theta}} . \tag{24}$$

The virtual control input is now obtained α_i:

$$\alpha_i = -z_{i-1} - c_i z_i + \sum_{k=1}^{i-1} \frac{\partial \alpha_{i-1}}{\partial x_k} x_{k+1} - \hat{\theta}^T (\varphi_i +$$

$$- \sum_{k=1}^{i-1} \frac{\partial \alpha_{i-1}}{\partial x_k} \varphi_k) + \sum_{k=1}^{i-1} \frac{\partial \alpha_{i-1}}{\partial y_r^{(k-1)}} \dot{y}_r^{(k)} +$$

$$+ \frac{\partial \alpha_{i-1}}{\partial \hat{\theta}} \Gamma \tau_i + \sum_{k=1}^{i-1} z_k \frac{\partial \alpha_{k-1}}{\partial \hat{\theta}} \Gamma (\varphi_i - \sum_{j=1}^{i-1} \frac{\partial \alpha_{i-1}}{\partial x_j} \varphi_j) , \tag{25}$$

where the constant c_i is positive and τ_i is the ith tuning function defined as

$$\tau_i = \tau_{i-1} + \left(\varphi_i - \sum_{k=1}^{i-1} \frac{\partial \alpha_{i-1}}{\partial x_k} \varphi_k \right) z_i . \tag{26}$$

The *Lyapunov* function candidate for the subsystem $(z_1, z_2 \ldots z_i)$ is defined by

$$V_i = V_{i-1} + \frac{1}{2} z_i^2 , \tag{27}$$

whose derivative along with (24) is

$$\dot{V}_i = -\sum_{k=1}^{i-1} c_k z_k^2 + z_i z_{i+1} + \tilde{\theta}^T \left(\tau_i - \Gamma^{-1} \dot{\hat{\theta}} \right) +$$

$$+ \left(\sum_{k=2}^{i} z_2 \frac{\partial \alpha_{k-1}}{\partial \hat{\theta}} \right) \left(\Gamma \tau_i - \dot{\hat{\theta}} \right) . \tag{28}$$

E. DEFINITION OF THE LAST ERROR VARIABLE z_n AND THE CONTROL LAW

Finally, the last error z_n and its corresponding derivative are defined by

$$z_n = x_n - y_r^{(n-1)} - \alpha_{n-1} , \tag{29}$$

$$\dot{z}_n = \varphi_0 + \beta u - \sum_{k=1}^{n-1} \frac{\partial \alpha_{n-1}}{\partial x_k} x_{k+1} + \theta^{*T} (\varphi_n +$$

$$- \sum_{k=1}^{n-1} \frac{\partial \alpha_{n-1}}{\partial x_k} \varphi_k) - \sum_{k=1}^{n-1} \frac{\partial \alpha_{n-1}}{\partial y_r^{k-1}} y_r^{(k)} - y_r^{(n)} - \frac{\partial \alpha_{n-1}}{\partial \hat{\theta}} \dot{\hat{\theta}} . \tag{30}$$

Hence, the control law u can be expressed as

$$u = \frac{1}{\beta} \left(\alpha_n + y_r^{(n)} \right) . \tag{31}$$

The virtual control entry α_n is given by

$$\alpha_n = -z_{n-1} - c_n z_n - \varphi_0 + \sum_{k=1}^{n-1} \frac{\partial \alpha_{n-1}}{\partial x_k} x_{k+1} +$$

$$- \hat{\theta}^T \left(\varphi_n - \sum_{k=1}^{n-1} \frac{\partial \alpha_{n-1}}{\partial x_k} \varphi_k \right) + \sum_{k=1}^{n-1} \frac{\partial \alpha_{n-1}}{\partial y_r}^{(k-1)} y_r^{(k)} +$$

$$+ \frac{\partial \alpha_{n-1}}{\partial \hat{\theta}} \Gamma \tau_n + \sum_{k=2}^{n-1} z_k \frac{\partial \alpha_{k-1}}{\partial \hat{\theta}} \Gamma \left(\varphi_n - \sum_{j=1}^{n-1} \frac{\partial \alpha_{n-1}}{\partial x_j} \varphi_j \right), \quad (32)$$

where the constant c_n is also positive and τ_n is the last tuning function defined as

$$\tau_n = \tau_{n-1} + \left(\varphi_n - \sum_{k=1}^{n-1} \frac{\partial \alpha_{n-1}}{\partial x_k} \varphi_k \right). \quad (33)$$

The candidate for the *Lyapunov* function and its respective derivative for the subsystem $(z_1, z_2 \ldots z_n)$ are

$$V_n = V_{n-1} + \frac{1}{2} z_n^2, \quad (34)$$

and

$$\dot{V}_n = -\sum_{k=1}^{n} c_k z_k^2 + \tilde{\theta}^T \left(\tau_n - \Gamma^{-1} \dot{\hat{\theta}} \right) + \left(\sum_{k=2}^{n} z_k \frac{\partial \alpha_{k-1}}{\partial \hat{\theta}} \right) \left(\Gamma \tau_n - \dot{\hat{\theta}} \right). \quad (35)$$

Finally, choosing

$$\dot{\hat{\theta}} = \Gamma \tau_n, \quad (36)$$

and replacing it into (35), we can show that

$$\dot{V}_n = -\sum_{k=1}^{n} c_k z_k^2 < 0. \quad (37)$$

As the function V_n is negative, the asymptotic stability of the tracking error of the variables z_i (considering $i = 1, \ldots, n$) and boundedness of the error of the estimated parameter $\tilde{\theta}$ are finally proved.

In order to avoid the partial derivatives in the traditional backstepping approach, as shown in this section, we will formulate in the next one our control problem using the modified version of this controller, as done in [18].

III. PROBLEM FORMULATION

Consider the nonlinear *strict-feedback* system, as described in equation (1).

The control objective is the same of section II.

In particular, the $y_r(t)$ reference is the output of a reference model with bounded and continuous input $r(t)$, or a signal whose first n derivatives are known, uniformly bounded and continuous by parts. Using the reference model paradigm, consider the following stable linear system

$$y_r(s) = \frac{k_m}{s^n + m_{n-1} s^{n-1} + \ldots + m_0} r(s), \quad (38)$$

where $s^n + m_{n-1} s^{n-1} + \ldots + m_0$ is a *Hurwitz* polynomial and the gain k_m is positive.

To achieve the control objective, the adaptive backstepping controller based on tuning functions [3] is used, but with the advantage of eliminating the partial derivatives in the controller structure.

Consider the following error variables in (39)–(40) and the stabilization functions in (41)–(42):

$$z_1 = x_1 - y_r, \quad (39)$$

$$z_i = x_i - y_r^{(i-1)} - \alpha_{i-1}, \quad (40)$$

$$\alpha_1 = -c_1 z_1 - \hat{\theta}^T \varphi_1, \quad (41)$$

$$\alpha_i = -c_i z_i - z_{i-1} - \hat{\theta}^T \varphi_i + \dot{\alpha}_{i-1}, \quad (42)$$

where c_i are positive constants and the tuning functions are given by

$$\tau_1 = \varphi_1 z_1, \quad \tau_i = \tau_{i-1} + \varphi_i z_i, \quad (43)$$

for $i = 2, \cdots, n$ and $\alpha_0 = z_0 = \tau_0 = 0$. In addition, the estimate of the parameter vector θ^* is obtained through the adaptation law

$$\dot{\hat{\theta}} = \Gamma \tau_n, \quad (44)$$

where $\Gamma > 0$ is the adaptation gain matrix.

Finally, we arrive at the control law based on state feedback:

$$u = \frac{1}{\beta} (\alpha_n + y_r^{(n)}), \quad (45)$$

where α_n is defined according to (42) for $i = n$ as

$$\alpha_n = -c_n z_n - z_{n-1} - \hat{\theta}^T \varphi_n + \dot{\alpha}_{n-1}. \quad (46)$$

Although the control law (45) seems to be simple, there is still an issue to be overcome: it is necessary to obtain the derivative of α_{n-1} that, *a priori*, is not available for the feedback design. To try to eliminate this obstacle, the exact differentiator with dynamic gain based on *higher-order sliding modes* (HOSM), as presented in [20], [25], [26], and [27], will be used. In this way, in addition to the exact differentiation, properties of global stability can be ensured.

IV. GLOBAL HOSM DIFFERENTIATOR WITH DYNAMIC GAIN

This section introduces the class of global HOSM differentiators that guarantee the exact differentiation of signals for arbitrary initial conditions. Since only the first derivative of each $\alpha_j(t), j = i - 1$, is necessary, the idea is to use the HOSM differentiator with dynamic gains $\mathcal{L}_j(x, \hat{\theta}, u, t)$ for each signal $\alpha_j \in \mathbb{R}, j = 1, \ldots, n-1$, as follows:

$$\dot{\zeta}_0^{i-1} = v_0^{i-1} = -\lambda_0^{i-1} \mathcal{L}_{i-1}^{1/2}(x, \hat{\theta}, u, t) |\zeta_0^{i-1} - \alpha_{i-1}|^{1/2}$$
$$\times sgn\left(\zeta_0^{i-1} - \alpha_{i-1}\right) + \zeta_1^{i-1}, \quad (47)$$

$$\dot{\zeta}_1^{i-1} = -\lambda_1^{i-1} \mathcal{L}_{i-1}(x, \hat{\theta}, u, t) sgn\left(\zeta_1^{i-1} - v_0^{i-1}\right), \quad (48)$$

where the $j = i - 1$ index is used to indicate which variable α_{i-1} is associated with the differentiator.

The difficulty in calculating the upper bound $\mathcal{L}_{i-1}$ for $\ddot{\alpha}_{i-1}$ is in the fact that $\ddot{\alpha}_{i-1}$ always depends on $\dot{\alpha}_{i-1}$. However, the next lemma shows that $\dot{\alpha}_i$ is indeed a function of the state x, of the estimate $\hat{\theta}$, and of the time variable t (due to the dependence of $y_r(t)$ and its derivatives up to order n), i.e., $\dot{\alpha}_i(x, \hat{\theta}, t)$. In particular, for $i = n$, the dependence on u will be explict as well. Therefore, due to the knowledge of the state of the plant and the reference model, it is possible to assume known functions that upper bound $\dot{\alpha}_i$, $\forall i = 1, \ldots, n$.

Lemma 1: There are known estimated upper bounds for signs $\dot{\alpha}_i$, $i = 1, \ldots, n$, so that

$$|\dot{\alpha}_i| \le \psi_i(x, \hat{\theta}, t), \quad \forall t > 0, \tag{49}$$

$$|\dot{\alpha}_n| \le \psi_n(x, \hat{\theta}, u, t), \quad \forall t > 0. \tag{50}$$

Proof: The proof will cover the calculations up to the definition of the signal $\dot{\alpha}_3$ in function of α_1 and their respective derivatives and is based on the equations in (42) rewritten below:

$$\alpha_1 = -c_1 z_1 - \hat{\theta}^T \varphi_1,$$
$$\alpha_i = -c_i z_i - z_{i-1} - \hat{\theta}^T \varphi_i + \dot{\alpha}_{i-1},$$

It's easy to see that α_2 is in function of $\dot{\alpha}_1$, so we will skip this step for calculating α_3:

$$\alpha_3 = -c_3 z_3 - z_2 - \hat{\theta}^T \varphi_3 + \dot{\alpha}_2, \tag{51}$$

$$\dot{\alpha}_2 = -c_2 \dot{z}_2 - \dot{z}_1 - \frac{d}{dt}(\hat{\theta}^T \varphi_2) + \ddot{\alpha}_1, \tag{52}$$

$$\alpha_3 = -c_3 z_3 - z_2 - \hat{\theta}^T \varphi_3 - c_2 \dot{z}_2 - \dot{z}_1 - \frac{d}{dt}(\hat{\theta}^T \varphi_2) + \ddot{\alpha}_1. \tag{53}$$

The same process is repeated for calculating α_4:

$$\alpha_4 = -c_4 z_4 - z_3 - \hat{\theta}^T \varphi_4 + \dot{\alpha}_3, \tag{54}$$

$$\dot{\alpha}_3 = -c_3 \dot{z}_3 - \dot{z}_2 - \frac{d}{dt}\hat{\theta}^T \varphi_3 - c_2 \ddot{z}_2 - \ddot{z}_1 - \frac{d^2}{dt^2}(\hat{\theta}^T \varphi_2) + \dddot{\alpha}_1, \tag{55}$$

$$\alpha_4 = -c_4 z_4 - z_3 - \hat{\theta}^T \varphi_4 - c_3 \dot{z}_3 - \dot{z}_2 - \frac{d}{dt}\hat{\theta}^T \varphi_3 +$$
$$- c_2 \ddot{z}_2 - \ddot{z}_1 - \frac{d^2}{dt^2}(\hat{\theta}^T \varphi_2) + \dddot{\alpha}_1. \tag{56}$$

Error variables (40) and their respective time derivatives can also be converted into functions dependent on α_1 and yours " $i - 1$" time derivatives:

$$z_1 = x_1 - y_r, \qquad \dot{z}_1 = \dot{x}_1 - \dot{y}_r, \qquad \ddot{z}_1 = \ddot{x}_1 - \ddot{y}_r, \tag{57}$$
$$z_2 = x_2 - \dot{y}_r - \alpha_1, \qquad \dot{z}_2 = \dot{x}_2 - \ddot{y}_r - \dot{\alpha}_1, \tag{58}$$
$$z_3 = x_3 - \ddot{y}_r - \alpha_2. \tag{59}$$

Replacing α_2 in (59) by an expression in function of α_1, we obtain

$$z_3 = x_3 - \ddot{y}_r + c_2 z_2 + z_1 + \hat{\theta}^T \varphi_2 - \dot{\alpha}_1, \tag{60}$$

$$\dot{z}_3 = \dot{x}_3 - \dddot{y}_r + c_2 \dot{z}_2 + \dot{z}_1 + \frac{d}{dt}\hat{\theta}^T \varphi_2 - \ddot{\alpha}_1. \tag{61}$$

And finally substituting the derivatives of the error variables, we have

$$\dot{z}_3 = \dot{x}_3 - \dddot{y}_r + c_2(\dot{x}_2 - \ddot{y}_r - \dot{\alpha}_1) + \dot{x}_1 - \dot{y}_r + \frac{d}{dt}\hat{\theta}^T \varphi_2 + -\ddot{\alpha}_1. \tag{62}$$

the expression in (56) is established in function only of the known variables, that is, of α_1 and their respective time derivatives, the state, the reference model and the adaptive law:

$$\alpha_4 = -c_4\big(x_4 - \dddot{y}_r - (-c_3(x_3 - \ddot{y}_r + c_2(x_2 - \dot{y}_r - \alpha_1) +$$
$$+ (x_1 - y_r) + \hat{\theta}^T \varphi_2 - \dot{\alpha}_1) - (x_2 - \dot{y}_r - \alpha_1) - \hat{\theta}^T \varphi_3 +$$
$$- c_2(\dot{x}_2 - \ddot{y}_r - \dot{\alpha}_1) - (\dot{x}_1 - \dot{y}_r) - \frac{d}{dt}(\hat{\theta}^T \varphi_2) + \ddot{\alpha}_1)) +$$
$$- (x_3 - \ddot{y}_r - (-c_2(x_2 - \dot{y}_r - \alpha_1) - x_1 + y_r) - \hat{\theta}^T \varphi_2 +$$
$$+ \dot{\alpha}_1) - \hat{\theta}^T \varphi_4 - c_3(\dot{x}_3 - \dddot{y}_r + c_2(\dot{x}_2 - \ddot{y}_r - \dot{\alpha}_1) + \dot{x}_1 +$$
$$- \dot{y}_r + \frac{d}{dt}\hat{\theta}^T \varphi_2 - \ddot{\alpha}_1) - (\dot{x}_2 - \ddot{y}_r - \dot{\alpha}_1) - \frac{d}{dt}\hat{\theta}^T \varphi_3 +$$
$$- c_2(\ddot{x}_2 - \dddot{y}_r - \ddot{\alpha}_1) - (\ddot{x}_1 - \ddot{y}_r) - \frac{d^2}{dt^2}(\hat{\theta}^T \varphi_2) + \dddot{\alpha}_1. \tag{63}$$

By construction, we can realize that the time derivative of each tuning function exhibits recursively the same structure:

$$\dot{\alpha}_1 = \underline{\psi}_1(x, \hat{\theta}, t) + f_1(\alpha_1), \tag{64}$$
$$\dot{\alpha}_2 = \underline{\psi}_2(x, \hat{\theta}, t) + f_2(\alpha_1, \dot{\alpha}_1, \ddot{\alpha}_1), \tag{65}$$
$$\dot{\alpha}_3 = \underline{\psi}_3(x, \hat{\theta}, t) + f_3(\alpha_1, \dot{\alpha}_1, \ddot{\alpha}_1, \dddot{\alpha}_1), \tag{66}$$
$$\dot{\alpha}_4 = \underline{\psi}_4(x, \hat{\theta}, t) + f_4(\alpha_1, \dot{\alpha}_1, \ddot{\alpha}_1, \dddot{\alpha}_1, \ddddot{\alpha}_1), \tag{67}$$
$$\vdots$$
$$\dot{\alpha}_i = \underline{\psi}_i(x, \hat{\theta}, t) + f_i(\alpha_1 \ldots \alpha_1^{(i)}), \tag{68}$$
$$\dot{\alpha}_{i+1} = \underline{\psi}_{i+1}(x, \hat{\theta}, t) + f_{i+1}(\alpha_1 \ldots \alpha_1^{(i+1)}), \tag{69}$$
$$\vdots$$
$$\dot{\alpha}_n = \underline{\psi}_n(x, \hat{\theta}, u, t) + f_n(\alpha_1 \ldots \alpha_1^{(n)}). \tag{70}$$

By mathematical induction, we finally arrive at the conclusion that every signal $\dot{\alpha}_i$ can be derived from known signals, i.e., $\dot{\alpha}_i(x, \hat{\theta}, t)$ and $\dot{\alpha}_n(x, \hat{\theta}, u, t)$. Hence, there exist known functions $\psi_i(x, \hat{\theta}, t)$ and $\psi_n(x, \hat{\theta}, u, t)$ which are indeed upper bounds for the right-hand sides of the equations (64)–(70), according to (49)–(50), respectively. ∎

Lemma 2: Consider the dynamic gain of the differentiator (47)–(48) defined by

$$\mathcal{L}_{i-1}(x, \hat{\theta}, u, t) := k_1^{i-1}\|x\| + k_2^{i-1}\|y_R\| + k_3^{i-1}|u| + \bar{\phi}(x, \hat{\theta}, t), \tag{71}$$

where $y_R^T = [\dot{y}_r, \ldots, y_r^{(n)}]$. In addition, $\bar{\phi}(x, \hat{\theta}, t)$ is a norm bound for both nonlinear terms $\varphi^T = [\varphi_1, \ldots, \varphi_n]$ and $\dot{\varphi}^T = [\dot{\varphi}_1, \ldots, \dot{\varphi}_n]$, while k_1^{i-1}, k_2^{i-1} and k_3^{i-1} are positive

constants. Thus, the following upper bound can be obtained, for some finite time $T > 0$:

$$|\ddot{\alpha}_{i-1}| \leq \mathcal{L}_{i-1}(x, \hat{\theta}, u, t), \quad \forall t \geq T. \quad (72)$$

Proof: It is not difficult to show that equation (42) can be rewritten as

$$\dot{\alpha}_{i-1} = c_i z_i + z_{i-1} + \hat{\theta}^T \varphi_i + \alpha_i, \quad (73)$$

whose time derivative is

$$\ddot{\alpha}_{i-1} = c_i \dot{z}_i + \dot{z}_{i-1} + \dot{\hat{\theta}}^T \varphi_i + \hat{\theta}^T \dot{\varphi}_i + \dot{\alpha}_i. \quad (74)$$

With help from equations (40), (42), (43), (44) and (73), we get

$$\begin{aligned}
\ddot{\alpha}_{i-1} &= c_i(\dot{x}_i - y_r^i - \dot{\alpha}_{i-1}) + (\dot{x}_{i-1} - y_r^{i-1} - \dot{\alpha}_{i-2}) + \\
&\quad + \dot{\hat{\theta}}^T \varphi_i + \hat{\theta}^T \dot{\varphi}_i + \dot{\alpha}_i \\
&= c_i(\dot{x}_i) + (x_i + \theta^{*T}\varphi_{i-1}) + \dot{\hat{\theta}}^T \varphi_i + \hat{\theta}^T \dot{\varphi}_i + \\
&\quad - c_i(y_r^i + \dot{\alpha}_{i-1}) - y_r^{i-1} - \dot{\alpha}_{i-2} + \dot{\alpha}_i \\
&= c_i(\dot{x}_i) + (x_i + \theta^{*T}\varphi_{i-1}) + \left[\Gamma\left(\sum_{k=1}^n \varphi_k z_k\right)\right]^T \varphi_i + \\
&\quad + \hat{\theta}^T \dot{\varphi}_i - c_i y_r^i - y_r^{i-1} - c_i \dot{\alpha}_{i-1} - \dot{\alpha}_{i-2} + \dot{\alpha}_i. \quad (75)
\end{aligned}$$

Now, the upper bound of (75) can be calculated using equations (49)-(50) and following the same analogy made in the proof of Lemma 1, that is, that both the stabilizing functions and the error functions are dependents of the state x, of the reference model y_r and of a constant:

$$\begin{aligned}
\ddot{\alpha}_{i-1} &\leq (c_i\beta)|u| + (c_i + 1)\|y_R\| + \|\theta^*\|\|\varphi\|(c_i + 1) + \\
&\quad + |x_i| + \|\Gamma\left(\sum_{k=1}^i \varphi_k z_k\right)\varphi_i\| + \|\hat{\theta}\|\|\dot{\varphi}_i\| + c_i\psi_{i-1} + \\
&\quad + \psi_{i-2} + \psi_i, \\
&\leq (c_i\beta)|u| + (c_i + 1)\|y_R\| + \bar{\theta}\|\varphi\|(c_i + 1) + |x_i| + \\
&\quad + \|\Gamma\|\|\varphi\|^2\left(p_1\|x\| + p_2\|y_R\| + \sum_{l=1}^i \psi_l(x, t)\right) + \\
&\quad + \|\hat{\theta}\|\|\dot{\varphi}\| + c_i\psi_{i-1} + \psi_{i-2} + \psi_i, \\
&\leq (c_i\beta)|u| + (c_i + 1)\|y_R\| + |x_i| + \bar{\theta}\|\varphi\|(c_i + 1) + \\
&\quad + \|\Gamma\|\|\varphi\|^2(p_1\|x\| + p_2\|y_R\|) + \sum_{l=1}^i \psi_l(x, t) + \\
&\quad + \|\hat{\theta}\|\|\dot{\varphi}\| + c_i\psi_{i-1} + \psi_{i-2} + \psi_i. \quad (76)
\end{aligned}$$

where p_1 and p_2 are constants depending on the order of the system and $\|\theta^*\| \leq \bar{\theta}$ the upper bound of the unknown term.

Defining the constants

$$\begin{cases}
k_1^{i-1} > 1, \\
k_2^{i-1} > (c_i + 1), \\
k_3^{i-1} > (c_i\beta),
\end{cases} \quad (77)$$

non-negative, one can obtain the upper bound for non-linear terms such as

$$\begin{aligned}
\bar{\phi}(x, \hat{\theta}, t) &> \bar{\theta}\|\varphi\|(c_i + 1) + \|\Gamma\|\|\varphi\|^2(p_1\|x\| + p_2\|y_R\|) + \\
&\quad + \sum_{l=1}^i \psi_l(x, t) + \|\hat{\theta}\|\|\dot{\varphi}\| + c_i\psi_{i-1} + \psi_{i-2} + \psi_i. \quad (78)
\end{aligned}$$

The inequality (72) can be further increased by

$$\ddot{\alpha}_{i-1} \leq k_1^{i-1}\|x\| + k_2^{i-1}\|y_R\| + k_3^{i-1}|u| + \bar{\phi}(x, \hat{\theta}, t). \quad (79)$$

Thus, the gains of the differentiator can be defined as in (71), such that (72) is satisfied. ∎

Lemma 2, therefore, proposes that the gain is independent of the stabilizing functions, which according to Lemma 1, are in function of $\psi_i(x, t)$ e $\psi_n(x, u, t)$. The stability proof of this differentiator will be presented below.

Lemma 3: *Consider the global HOSM differentiator (47)–(48) with dynamic gains (71) satisfying (72). If the parameters $\lambda_j^{i-1} > 0$ are chosen recursively, the following equalities*

$$\zeta_0^{i-1}(t) = \alpha_{i-1}(t), \qquad \zeta_1^{i-1}(t) = \dot{\alpha}_{i-1}(t), \quad (80)$$

are globally satisfied in finite time.

Proof: In a similar way to that presented in [28], one can find *Lyapunov* function of the auxiliary estimation error $\bar{z} = \frac{\alpha_{i-1} - \zeta_1^{i-1}}{\mathcal{L}_{i-1}}$, $i = 1, \ldots, n-1$, whose time derivative satisfies, for some constant $k > 0$, the following inequality

$$\dot{V} \leq -kV(\bar{z})^{\frac{p-1}{p}} - \frac{\dot{\mathcal{L}}_{i-1}}{\mathcal{L}_{i-1}}\gamma(\dot{\mathcal{L}}_{i-1})V(\bar{z}), \quad (81)$$

where

$$\gamma(\dot{\mathcal{L}}_{i-1}) = \begin{cases}
\gamma_1 & if \quad \dot{\mathcal{L}}_{i-1} \geq 0 \quad or \\
\gamma_2 & if \quad \dot{\mathcal{L}}_{i-1} < 0, \quad 0 < \gamma_1 < \gamma_2.
\end{cases}$$

Thus, three cases can be admitted:

- The gain $\mathcal{L}_{i-1}$ is constant. This case is addressed in [19].
- The gain $\mathcal{L}_{i-1}$ is differentiable and grows at the most exponentially ($\frac{|\dot{\mathcal{L}}_{i-1}|}{|\mathcal{L}_{i-1}|} \leq M_{i-1}$) for a given constant $M_{i-1} > 0$. This case is addressed in [29].
- The gain $\mathcal{L}_{i-1}$ is differentiable and grows unboundedly ($\dot{\mathcal{L}}_{i-1} \geq 0$). The system is globally stable in finite time, according to [28].

In closed loop, the differentiator converges and the control signal leads the system to the equilibrium. Thus, the gain decreases and enters into a compact region where all the results of [19] or [29] can also be invoked. So, the convergence of (80) can be guaranteed through the use of the same arguments and statements in [19], [28], and [29].

In all the cases, thus (80) is satisfied in finite time. ∎

It is important to clarify that although we assume the complete measurement of plant state, we still need to find a norm bound for $\ddot{\alpha}_{i-1}$—see inequality (72) in Lemma 2, which will be employed to construct the dynamic gain (71) of the HOSM differentiator (47) and (48), for ultimately

obtaining an exact estimate of $\dot{\alpha}_{i-1}$, according to (80) in Lemma 3. The latter will be used in the derived control law (45) and (46), for $i = n$. The crucial point here is to realize that the computation of $\ddot{\alpha}_{i-1}$ depends on the unknown signal $\dot{\alpha}_i$, according to the expression (75) in the proof of Lemma 2. However, at this point we do not need to know exactly $\dot{\alpha}_i$. We just need to find an upper bound for that. To this end, Lemma 1 shows that implementable upper bounds for $|\dot{\alpha}_i|$ can be assured, for all $i = 1, \ldots, n$. Such upper bounds are functions of the measurable signals $x(t)$, $\hat{\theta}(t)$, and $y_R(t) = [\dot{y}_r(t), \ldots, y_r^{(n)}(t)]^T$, as shown in inequalities (49) and (50) of Lemma 1.

V. GLOBAL HOSM DIFFERENTIATOR-BASED BACKSTEPPING CONTROL

In this section, it is shown that the Adaptive *Backstepping* Control via Tuning Functions presented in Section II can be redesigned. Since the exact estimates of the derivatives $\dot{\alpha}_{i-1}$ can be obtained using the global differentiator presented in Section III. Basically, the change is to use stabilization functions of the type

$$\alpha_1 = -c_1 z_1 - \hat{\theta}^T \varphi_1, \quad \alpha_i = -c_i z_i - z_{i-1} - \hat{\theta}^T \varphi_i + \zeta_1^{i-1}. \tag{82}$$

The block diagram on Figure 2 and the Table 1 represent the summary of the proposed control method. In the following theorem, the main stability results are presented.

Theorem 1: Consider the plant (1), error variables (40), tuning functions in (43), adaptation law (44), control law (45), global HOSM differentiators (47)–(48) with dynamic gains (71) satisfying (72) and the stabilization functions (82). Hence, for any initial condition, all closed-loop signals are globally uniformly bounded, and the tracking of the system output $y(t)$, in relation to the reference signal $y_r(t)$ is achieved asymptotically.

Proof: The proof is divided into a few steps. We will first prove that the exact estimates of $\dot{\alpha}_{i-1}$ are indeed obtained in finite time, according to Lemma 3.

Step 1: From Lemma 2, it is possible to conclude that each dynamic gain $\mathcal{L}_{i-1}$ from the differentiators (47) and (48) satisfy the conditions introduced in [28] and [29] in finite time.

Thus, there are finite-time instants $T_j > 0$ for each α_j such that inequality (72) is satisfied, $\forall t > \max\{T_1, \ldots, T_{n-1}\}$. Then, the errors of the differentiators are forced to reach a compact set in which the conditions given in [28] and [29] can be invoked and it follows that equation (80) is satisfied. Consequently, the derivative of the stabilization function $\dot{\alpha}_{i-1}$ is exactly estimated, that is, $\zeta_1^{i-1} \equiv \dot{\alpha}_{i-1}$. Since this equality is achieved after a finite time $t > T$, being $T := \max\{T_1, \ldots, T_{n-1}\}$, the next steps of the proof will be the same as in [18].

Step 2: Consider the output error (39) and its derivative through (1), given by

$$\dot{z}_1 = x_2 + \theta^{*T} \varphi_1(x_1) - \dot{y}_r. \tag{83}$$

Replacing $x_2 = z_2 + \dot{y}_r + \alpha_1$ in (40) for $i = 2$, we have

$$\dot{z}_1 = z_2 + \alpha_1 + \theta^{*T} \varphi_1. \tag{84}$$

Now, considering the estimation error

$$\tilde{\theta} = \theta^* - \hat{\theta}, \tag{85}$$

the *Lyapunov* function candidate for calculating the system stability of $(z_1, \tilde{\theta})$ is given by

$$V_1 = \frac{1}{2} z_1^2 + \frac{1}{2} \tilde{\theta}^T \Gamma^{-1} \tilde{\theta}, \tag{86}$$

and its derivative, through (84) and (85), is given by

$$\dot{V}_1 = z_1 \left(z_2 + \alpha_1 + \hat{\theta}^T \varphi_1 \right) - \tilde{\theta}^T \Gamma^{-1} \left(\dot{\hat{\theta}} - \Gamma \varphi_1 z_1 \right). \tag{87}$$

Choosing the stabilization function

$$\alpha_1 = -c_1 z_1 - \hat{\theta}^T \varphi_1, \tag{88}$$

the following expression is obtained

$$\dot{V}_1 = -c_1 z_1^2 + z_1 z_2 + \tilde{\theta}^T \left(\tau_1 - \Gamma^{-1} \dot{\hat{\theta}} \right), \tag{89}$$

where the first tuning function is simply

$$\tau_1 = \varphi_1 z_1. \tag{90}$$

Step 3: Supposing the error z_2 in (40) and calculating its derivative using (1), we get

$$\dot{z}_2 = x_3 + \theta^{*T} \varphi_2(x_1, x_2) - \ddot{y}_r - \dot{\alpha}_1. \tag{91}$$

Replacing $x_3 = z_3 + \ddot{y}_r + \alpha_2$ obtained in (40) and $\dot{\alpha}_1$ for ζ_1^1 via (80), we get

$$\dot{z}_2 = z_3 + \alpha_2 + \theta^{*T} \varphi_2 - \zeta_1^1. \tag{92}$$

The new *Lyapunov* function candidate is

$$V_2 = V_1 + \frac{1}{2} z_2^2, \tag{93}$$

and its derivative

$$\dot{V}_2 = -c_1 z_1^2 + z_2 \left(z_1 + z_3 + \alpha_2 + \hat{\theta}^T \varphi_2 - \zeta_1^1 \right) + \\ + \tilde{\theta}^T \left(\tau_1 + \varphi_2 z_2 - \Gamma^{-1} \dot{\hat{\theta}} \right), \tag{94}$$

using (85), (89) and (92). Selecting the stabilization function

$$\alpha_2 = -c_2 z_2 - z_1 + \zeta_1^1 - \hat{\theta}^T \varphi_2, \tag{95}$$

we have the expession

$$\dot{V}_2 = -c_1 z_1^2 - c_2 z_2^2 + z_2 z_3 + \tilde{\theta}^T \left(\tau_2 - \Gamma^{-1} \dot{\hat{\theta}} \right), \tag{96}$$

where the second tuning function is written as

$$\tau_2 = \tau_1 + \varphi_2 z_2. \tag{97}$$

Step i: The error z_i has it's general expression (40) and its derivative by means of (1) changing $\dot{\alpha}_{i-1}$ by ζ_1^{i-1} along with (80), leads to

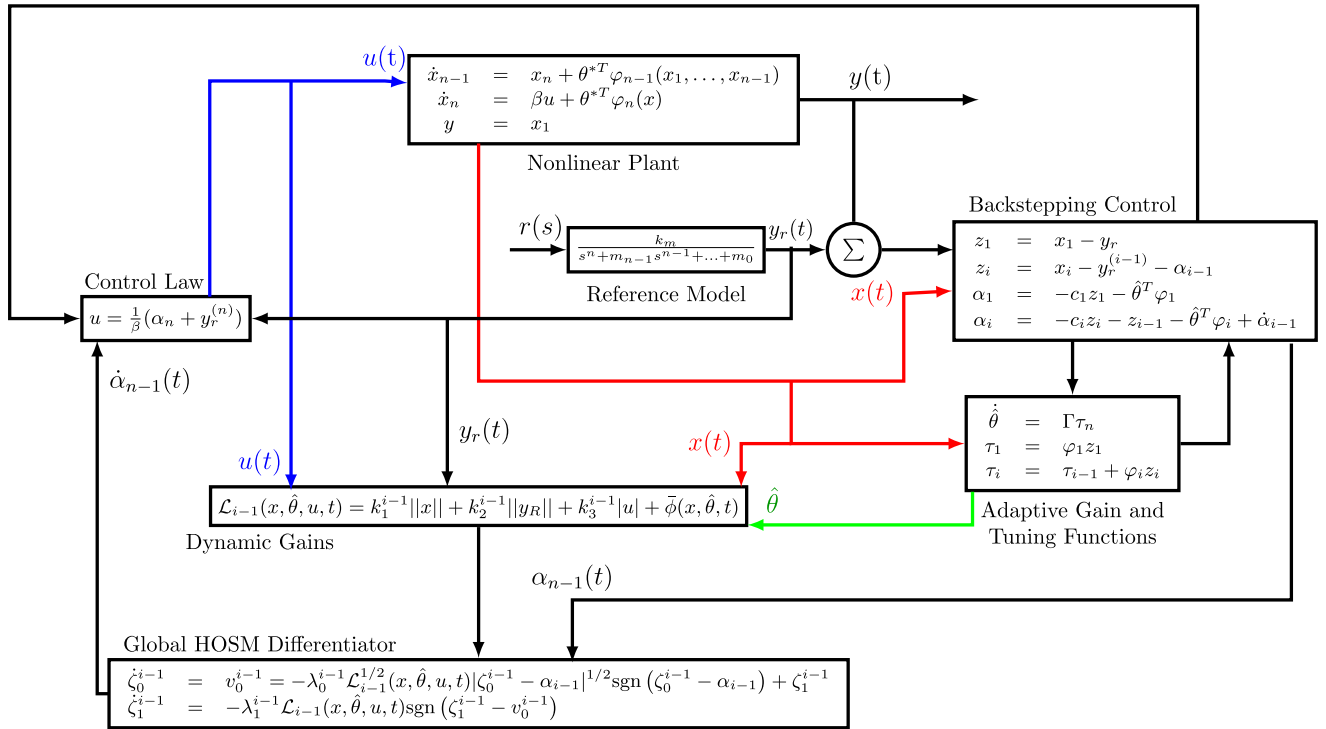$$\dot{z}_i = x_{i+1} + \theta^{*T} \varphi_i(x_1, \ldots, x_i) - y_r^{(i)} - \zeta_1^{i-1}. \tag{98}$$

FIGURE 2. Adaptive Backstepping control based on a Global HOSM Differentiator with Adaptive Gains.

TABLE 1. Summary of the main closed-loop equations.

SISO Plant	$\dot{x}_i = x_{i+1} + \theta^{*T}\varphi_i(x_1,\ldots,x_i)\,,\quad i = 1,\ldots,n-1\,,$ $\dot{x}_n = \beta u + \theta^{*T}\varphi_n(x)\,,$ $y = x_1\,.$
Unknown Parameters	$\theta^* \in \mathbb{R}^p$
Reference Model	$y_r(s) = \frac{k_m}{s^n + m_{n-1}s^{n-1} + \ldots + m_0} r(s)$
Estimate of the Parameters Vector	$\dot{\hat{\theta}} = \Gamma\tau_n$
Control Law	$u = \frac{1}{\beta}\left(\alpha_n + y_r^{(n)}\right)$
Error Variables	$z_1 = x_1 - y_r\,,\quad z_i = x_i - y_r^{(i-1)} - \alpha_{i-1}$
Stabilization Functions	$\alpha_1 = -c_1 z_1 - \hat{\theta}^T\varphi_1\,, \alpha_i = -c_i z_i - z_{i-1} - \hat{\theta}^T\varphi_i + \dot{\alpha}_{i-1}$
Tuning Functions	$\tau_1 = \varphi_1 z_1\,,\quad \tau_i = \tau_{i-1} + \varphi_i z_i$
Global HOSM Differentiator	$\dot{\zeta}_0^{i-1} = v_0^{i-1} = -\lambda_0^{i-1}\mathcal{L}_{i-1}^{1/2}(x,\hat{\theta},u,t)\lvert\zeta_0^{i-1} - \alpha_{i-1}\rvert^{1/2}\mathrm{sgn}\left(\zeta_0^{i-1} - \alpha_{i-1}\right) + \zeta_1^{i-1}\,,$ $\dot{\zeta}_1^{i-1} = -\lambda_1^{i-1}\mathcal{L}_{i-1}(x,\hat{\theta},u,t)\mathrm{sgn}\left(\zeta_1^{i-1} - v_0^{i-1}\right)\,.$
Dynamic Gain of the HOSM Diff.	$\mathcal{L}_{i-1}(x,\hat{\theta},u,t) = k_1^{i-1}\lVert x\rVert + k_2^{i-1}\lVert y_R\rVert + k_3^{i-1}\lvert u\rvert + \bar{\phi}(x,\hat{\theta},t)$

Replacing $x_{i+1} = z_{i+1} + y_r^{(i)} + \alpha_i$ obtained in (40) for $i = i+1$, we get

$$\dot{z}_i = z_{i+1} + \alpha_i + \varphi_i^T\theta - \zeta_1^{i-1}\,. \tag{99}$$

Now, the *Lyapunov* function candidate is

$$V_i = V_{i-1} + \frac{1}{2}z_i^2, \tag{100}$$

and its derivative can be calculated as:

$$\dot{V}_i = -\sum_{k=1}^{i-1} c_k z_k^2 + z_i\left(z_{i-1} + z_{i+1} + \alpha_i + \varphi_i^T\hat{\theta} + \right.$$
$$\left. - \zeta_1^{i-1}\right) + \tilde{\theta}^T\left(\tau_{i-1} + \varphi_i z_i - \Gamma^{-1}\dot{\hat{\theta}}\right)\,. \tag{101}$$

Finally, the choice of the stabilization function

$$\alpha_i = -c_i z_i - z_{i-1} - \varphi_i^T\hat{\theta} + \zeta_1^{i-1}, \tag{102}$$

results in the expression

$$\dot{V}_i = -\sum_{k=1}^i c_k z_k^2 + z_i z_{i+1} + \tilde{\theta}^T\left(\tau_i - \Gamma^{-1}\dot{\hat{\theta}}\right), \tag{103}$$

where the general tuning function is

$$\tau_i = \tau_{i-1} + \varphi_i z_i. \tag{104}$$

Step n: Considering the last error z_n in (40), its derivative along with (1) and the change of $\dot{\alpha}_{n-1}$ by ζ_1^{n-1}, with the help

of (80), generates

$$\dot{z}_n = \beta(x)u + \varphi_n(x)^T\theta - y_r^{(n)} - \zeta_1^{n-1}. \quad (105)$$

The last *Lyapunov* function candidate is

$$V_n = V_{n-1} + \frac{1}{2}z_n^2, \quad (106)$$

with time-derivative

$$\dot{V}_n = -\sum_{k=1}^{n-1} c_k z_k^2 + z_n\Big(z_{n-1} + \beta u + \varphi_n^T\hat{\theta} + \\ - y_r^{(n)} - \zeta_1^{n-1}\Big) + \tilde{\theta}^T\Big(\tau_{n-1} + \varphi_n z_n - \Gamma^{-1}\dot{\hat{\theta}}\Big). \quad (107)$$

Finally, the control law defined as

$$u = \frac{1}{\beta}\Big(-c_n z_n - z_{n-1} - \varphi_n^T\hat{\theta} + \zeta_1^{n-1} + y_r^{(n)}\Big), \quad (108)$$

guarantees the global stability of the complete closed-loop system since

$$\dot{V}_n = -\sum_{k=1}^{n} c_k z_k^2 + \tilde{\theta}^T\Big(\tau_n - \Gamma^{-1}\dot{\hat{\theta}}\Big), \quad (109)$$

where the last tuning function is given by

$$\tau_n = \tau_{n-1} + \varphi_n z_n. \quad (110)$$

By plugging the parameter adaptation law

$$\dot{\hat{\theta}} = \Gamma\tau_n, \quad (111)$$

into (109), we get

$$\dot{V}_n = -\sum_{k=1}^{n} c_k z_k^2. \quad (112)$$

Thus, $[z^T, \tilde{\theta}^T]^T = [0, 0]^T$ is a globally uniformly stable equilibrium point. Moreover, using the theorem of *LaSalle-Yoshizawa* [30], it can be concluded that the errors $z_i \to 0$ as $t \to \infty$. ∎

VI. SIMULATION RESULTS

In this section, some simulation results for a third-order nonlinear system will be presented. The phenomenon presented here is the *Wing Rock*[1] which corresponds to the existence of a limit cycle on the longitudinal axis of a high-speed performance aircraft. The example proposed in this section is similar to that described in the work of Krstić et al. [3, page 180].

[1]Watch the online videos available by NASA at:
https://www.youtube.com/watch?v=6EOo7jJ8Phg
https://www.youtube.com/watch?v=JcFd0o-LtUU.
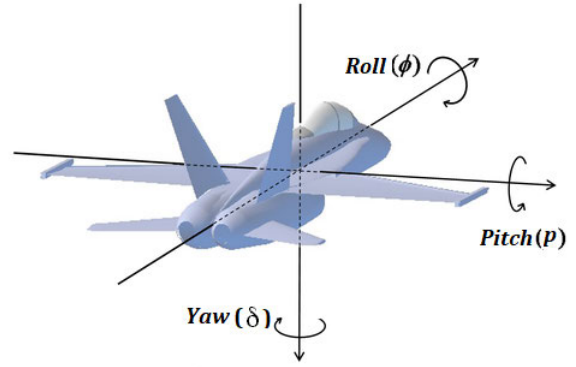
FIGURE 3. High performance plane with angles ϕ, p, δ. Image adapted from https://images.app.goo.gl/GyAYQTzedvucavB76 (last view in 15/07/2021).

A. APPLICATION TO WING ROCK CONTROL

Consider the third-order system with $x = [\phi, p, \delta_A]^T$:

$$\dot{\phi} = p,$$
$$\dot{p} = \delta_A + \theta^{*T}\varphi(\phi, p),$$
$$\dot{\delta}_A = \frac{1}{\tau}u - \frac{1}{\tau}\delta_A,$$
$$y = \phi. \quad (113)$$

The vector $\varphi(\phi, p) = [1, \phi, p, |\phi|p, |p|p]^T$ represents the nonlinearity of the system as a function of the state, $\theta^* = [\theta_1, \theta_2, \theta_3, \theta_4, \theta_5]^T$ are the unknown parameters and y is the output of the system. The reference model adopted is $y_r(s) = \frac{1}{(s+10)(s^2+4s+24.25)}r(s)$. The entry is $r(s) = 0$. The goal is to drive the system smoothly to the origin with a performance specified by the reference model. In this example, only the derivative of α_2 need to be estimated with the global HOSM differentiator (47)–(48) with dynamic gain (71):

$$\dot{\zeta}_0 = v_0 = -\lambda_0\mathcal{L}_2^{\frac{1}{2}}|\zeta_0 - \alpha_2|^{\frac{1}{2}}\text{sgn}(\zeta_0 - \alpha_2) + \zeta_1, \quad (114)$$
$$\dot{\zeta}_1 = -\lambda_1\mathcal{L}_2\text{sgn}(\zeta_1 - v_0). \quad (115)$$

The differentiator has dynamic gain given by

$$\mathcal{L}_2(x, \hat{\theta}, u, t) := k_1^2|\delta| + k_2^2\|y_r\| + k_3^2|u| + \bar{\phi}(x, \hat{\theta}, t), \quad (116)$$

with the following constants:

$$k_1^2 = \frac{c_2}{\tau} + c_2 c_1 + 1 + \frac{c_1}{\tau}, \quad (117)$$
$$k_2^2 = c_2 + c_1 + c_2 c_1 + 1, \quad (118)$$
$$k_3^2 = \frac{c_2}{\tau} + \frac{c_1}{\tau}, \quad (119)$$

and with the upper bound $\bar{\phi}$ for the nonlinear terms defined as

$$\bar{\phi} = (c_2 + c_1)\bar{\theta}\|\dot{\varphi}\| + (c_1 c_2 + 1 + \|\Gamma\|\|\varphi\|^2)\bar{\theta}\|\varphi\| + \\ + \|\hat{\theta}\|\|\ddot{\varphi}\| + \|\Gamma\|\Big(\|\dot{\varphi}\|\|\varphi\|\Big[|p| + |\dot{y}_r| + c_1(|\phi| +$$

$$+ |y_r|) \Big] + \|\varphi\|^2 \Big[|\delta| + |\ddot{y}_r| + c_1(|p| + |\dot{y}_r|) \Big] \Big) +$$

$$+ 2\Gamma \|\dot{\varphi}\| \Big(\|\varphi\| \big[|p| + |\dot{y}_r| + c_1(|\phi| + |y_r|) \big] \Big), \quad (120)$$

being $\|\theta^*\| \leq \bar{\theta}$ the norm bound of the unknown vector θ^*. In this example, it was not necessary to use the know ledge of the upper bounds for the known signals, as suggested in Lemma 1.

The errors variables are:

$$z_1 = \phi - y_r,$$
$$z_2 = p - \dot{y}_r - \alpha_1, \quad (121)$$
$$z_3 = \delta_A - \ddot{y}_r - \alpha_2,$$

where as the stabilization functions obtained with the help of the global HOSM differentiator are

$$\alpha_1 = -c_1 z_1,$$
$$\alpha_2 = -c_2 z_2 - z_1 - \hat{\theta}^T \varphi + \zeta_1^1. \quad (122)$$

Finally, the control law and then the adaptivation law are given by:

$$u = \tau \left(-c_3 z_3 - z_2 + \frac{1}{\tau} \delta_A + \zeta_1^2 + \ddot{y}_r \right), \quad (123)$$

$$\dot{\hat{\theta}} = \Gamma \tau_2 = \Gamma \varphi z_2. \quad (124)$$

The initial adopted conditions were $\phi(0) = 0.5$, $p(0) = \delta(0) = 0$, while the unknown parameters θ^* in the system were chosen as $\theta^* = [0, -26.67, 0.76, -2.92, 0]^T$, the constant $\tau = 0,67$, the adaptivation gain $\Gamma = 0.02I$, with the identity matrix denoted by I. The initial conditions of the estimated parameter $\hat{\theta}(0) = [0, -36.00, 1.03, -3.94, 0]^T$, the control parameters $c_1 = c_2 = c_3 = 5$ and the diferentiator constants are $\lambda_0^2 = 1.5$, $\lambda_1^2 = 1.1$ and $\bar{\theta} = 30$. The numerical integration procedure for solving ordinary differential equations was the Euler method and the integration step was chosen as $h = 10^{-4}s$. The simulation results can be seen in Figures 4, 5, 6 and 7.
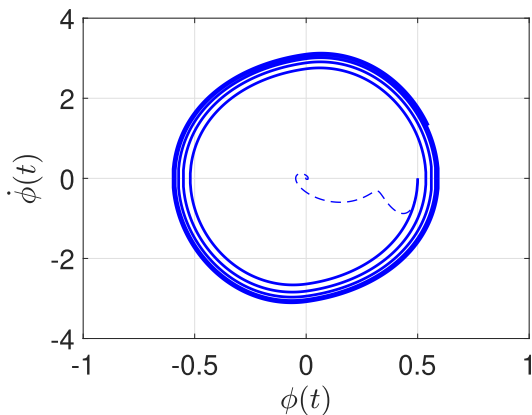
FIGURE 4. Phase plane for the open-loop (solid line) and closed-loop (dashed line) systems.
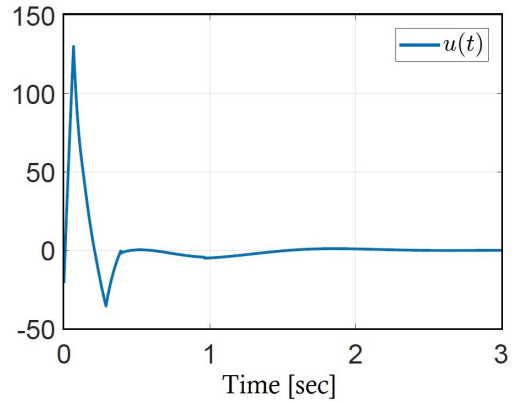
FIGURE 5. Control signal of the proposed adaptive controller *backstepping* for the *Wing Rock* system.
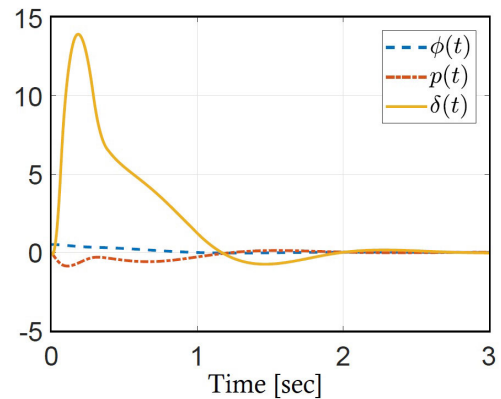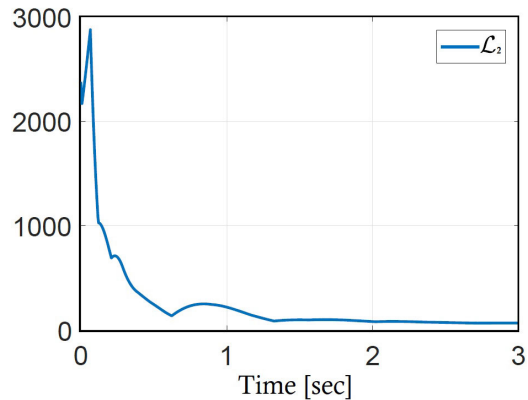

FIGURE 6. State variables.

FIGURE 7. Dynamic gain of the proposed exact *HOSM* differentiator.

B. COMPARISONS WITH OTHER DIFFERENTIATORS UNDER MEASUREMENT NOISE AND DELAYED SIGNALS

In order to numerically compare the developed adaptive backstepping control law with two other differentiator-based schemes, we consider in the next results real-world imperfections, such as noises and delays. It is used as a noise signal the sinusoidal function with amplitude 0.05 and frequency $1000 rad/sec$, and a delay of $0.1 sec$ in the measured signals $\phi(t)$ and $\delta_A(t)$ employed for the control design.

1) GLOBAL HOSM DIFFERENTIATOR WITH DYNAMIC GAINS

Even under delays and measurement noise, the proposed global *HOSM* differentiator with dynamic gain maintain the basic properties of the control law leading to the convergence of the output signal to the desired trajectory. The simulation plots can be seen in Figures 8, 9 and 10.
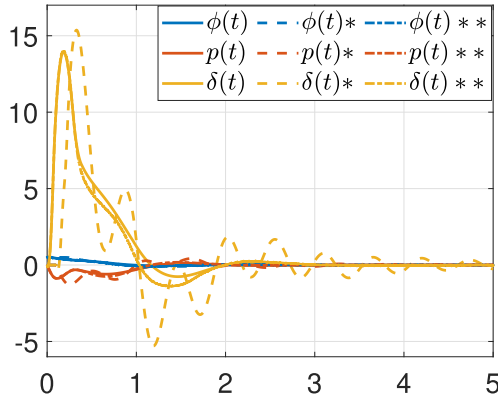

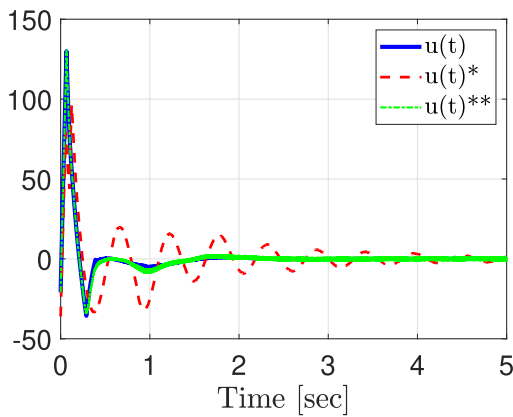**FIGURE 8.** State variables of the *Wing Rock* system under *delays, **noise and no imperfections using the Global HOSM differentiator with dynamic gains.

FIGURE 9. Control signal of the proposed Global HOSM differentiator with dynamic gains for the *Wing Rock* system under *delays, **noise and no imperfections.
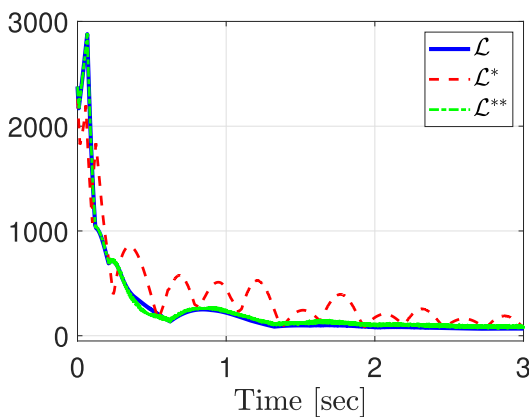
FIGURE 10. Dynamic gain of the proposed Global *HOSM* differentiator on the *Wing Rock* system under *delays, **noise and no imperfections.

2) LINEAR DIFFERENTIATOR

Also called lead filter, the linear (inexact) differentiator is based on the following first-order transfer function:

$$y_{out}(t) = \frac{s}{\tau_f s + 1} f(t), \tag{125}$$

where $y_{out}(t)$ corresponds to the output, τ_f is the time constant of the filter and the input $f(t)$ is the signal to be differentiated. The use of this differentiator requires a very low $0 < \tau_f \ll 1$, tending to zero so that the error between the output (estimate of the derivative) and the ideal (exact) value also approaches to zero. The control law, despite meeting the control objective, takes a huge effort due to the occurrence of the peaking phenomenon [31]. The simulation results can be seen in Figures 11, 12 and 13.
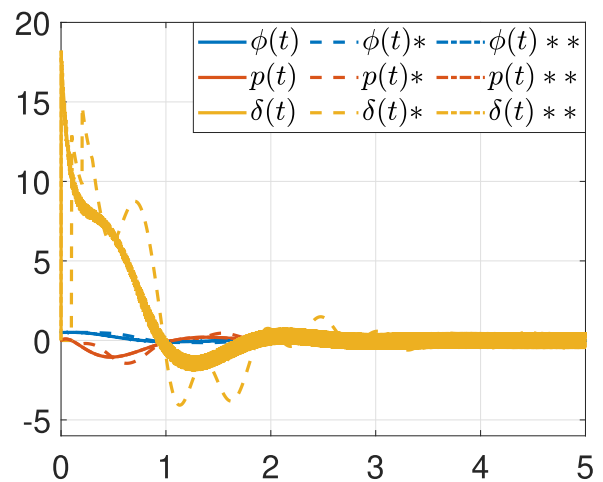

FIGURE 11. State variables of the *Wing Rock* system under *delays, **noise and no imperfections using the linear differentiator.
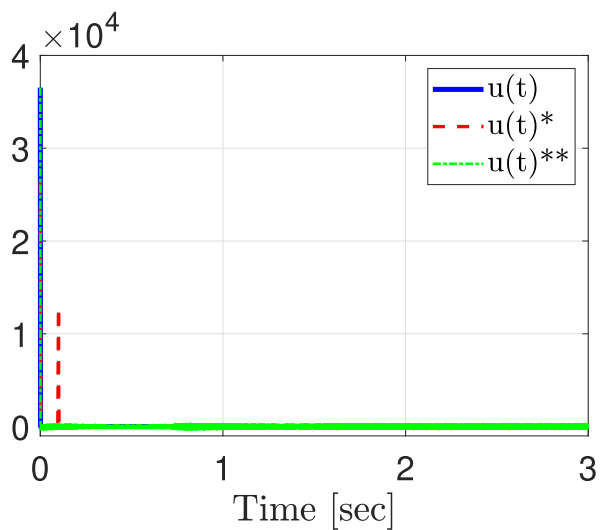

FIGURE 12. Control signal of the adaptive backstepping with linear differentiator for the *Wing Rock* system under *delays, **noise and no imperfections.
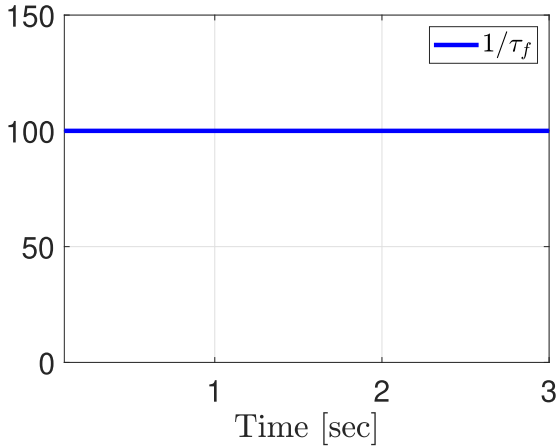
FIGURE 13. The same fixed gain ($1/\tau_f = 100$) of the lead filter used for the three studied cases: under *delays, with **noise, and without imperfections.

3) HOSM DIFFERENTIATOR WITH FIXED GAINS

Based on the algorithm described in [17] and [18], the following *HOSM* differentiator with fixed gain—also called Robust Exact Differentiatior (RED)—can be employed to estimate the base signal $\alpha_2(t)$ (whose second derivative has a local *Lipschitz* constant equal to $C_{[2]} > 0$) according to:

$$\dot{\zeta}_0^{[2]} = v_0^{[2]} = -\lambda_0^{[2]} C_{[2]}^{1/2} \left|\zeta_0^{[2]} - \alpha_{[2]}\right|^{1/2} \text{sgn}\left(\zeta_0^{[2]} - \alpha_{[2]}\right) + \zeta_1^{[2]},$$
(126)

$$\dot{\zeta}_1^{[2]} = -\lambda_1^{[2]} C_{[2]} \text{sgn}\left(\zeta_1^{[2]} - v_0^{[2]}\right).$$
(127)

The algorithm guarantees that $\zeta_0^{[2]}(t) = \alpha_{[2]}(t)$, $\zeta_1^{[2]}(t) = \dot{\alpha}_{[2]}(t)$ if

$$\left|\ddot{\alpha}_{[2]}\right| \leq C_{[2]}, \quad \forall t \geq T,$$
(128)

is at least locally satisfied, with some finite $T > 0$. In this differentiator, the state must be confined to a region of the state space and therefore does not apply to any initial condition, with exceptions, when, for example, the closed-loop system is homogeneous: local results imply global results [29].
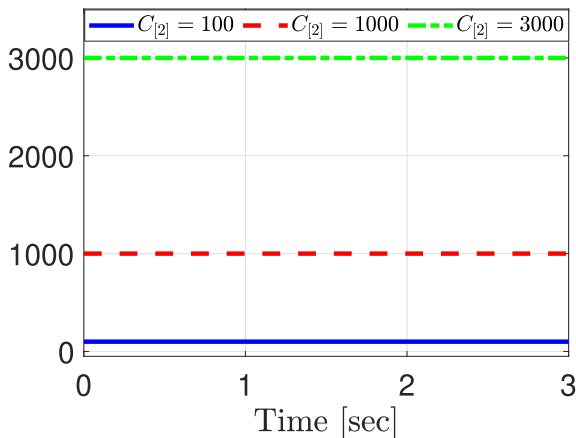

FIGURE 14. Selected gains of the HOSM differentiator with fixed gains on the *Wing Rock* system over time.

In the simulations, the constant $C_{[2]}$ was considered equal to 100 (the gain of the lead filter), 1000 (a mid term value) and 3000 (approximately the highest value of the dynamic gain found in Figure 10). The simulation results can be seen respectively in Figures 14 to 20.
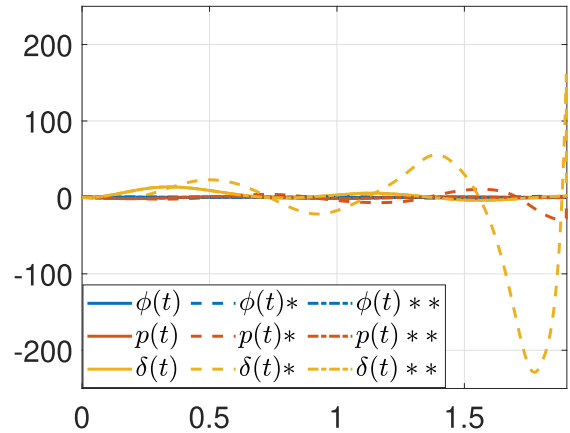

FIGURE 15. Unstable system with state variables of the *Wing Rock* system with HOSM differentiator with fixed gain $C_{[2]} = 100$ over time.
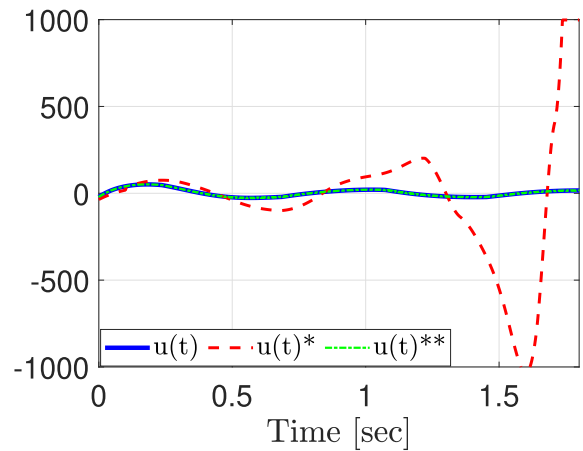

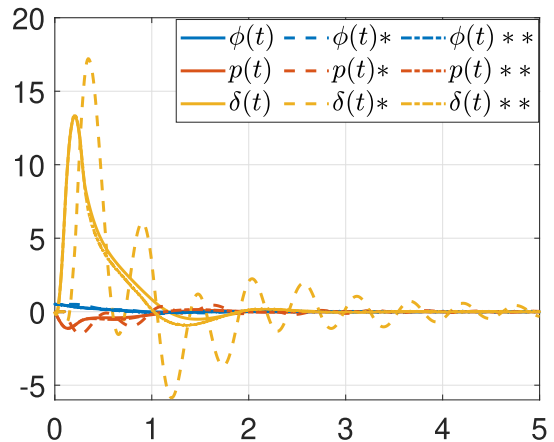**FIGURE 16.** Unstable system with control signal of the HOSM differentiator with fixed $C_{[2]} = 100$.

FIGURE 17. State variables of the *Wing Rock* system with HOSM differentiator with fixed $C_{[2]} = 1000$.
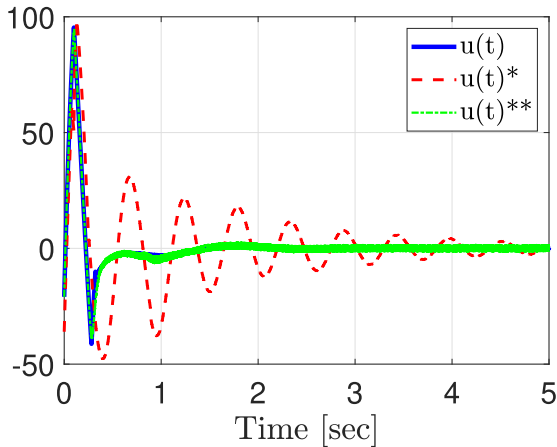
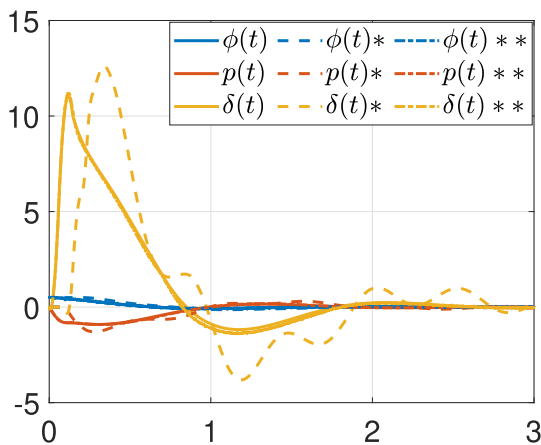**FIGURE 18.** Control signal of the HOSM differentiator with fixed $C_{[2]} = 1000$.

FIGURE 19. State variables of the *Wing Rock* system with HOSM differentiator with fixed $C_{[2]} = 3000$.
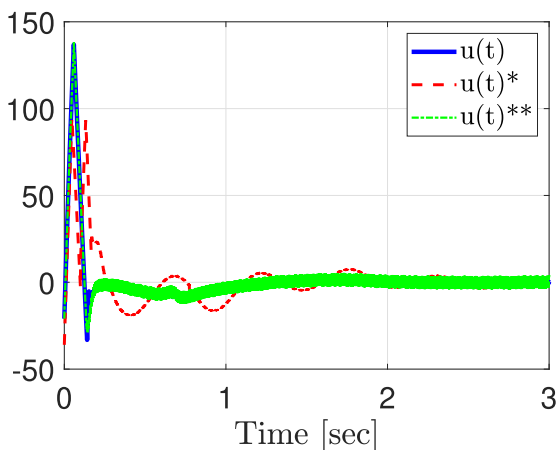

FIGURE 20. Control signal of the HOSM differentiator with fixed $C_{[2]} = 3000$.

In addition to being valid only locally, the main disadvantage of the HOSM differentiator with fixed gain, as the name itself says, is that the gain is fixed and therefore does not decrease with time as happens in the dynamic gain according, to Figure 10. Thus, the HOSM differentiator with fixed gain may be more sensitive to measurement noise in practical applications.

VII. EXPERIMENTAL RESULTS WITH A DC MOTOR

An experimental evaluation of the proposed method is showed below. Here, we restrict ourselves to some of the considered relative degree compensation schemes.

The experiments were performed using a laboratory prototype (Figures 21 and 22) based on a permanent magnet DC motor 2342024CR with built in gear box (1 : 43), from MicroMo Electronics, Inc., of the Quanser Consulting Plant SRV-02. The control algorithm was implemented on a motion control system based on a digital signal processor (DSP) hosted in a microcomputer.

The control signal u is the armature voltage, which is generated by a 12-bit digital-to-analog converter connected to a linear power amplifier (motor driver). The sampling frequency is 2.5 kHz. The motor angular position is measured by an incremental optical encoder with resolution 1000 *counts per revolution* (cpr). The resolution of the measured angular position of the load is 172000 cpr due to the gear box and the electronics on the card.

The following nominal relative degree two model of the DC motor is used, neglecting the small electrical time constant

$$G(s) = \frac{y}{u} = \frac{k_p}{s(s + 10)}, \tag{129}$$

where y is the angular position in degrees, u is the armature voltage in volts and the gain $k_p \in [600, 1000]$ is uncertain.

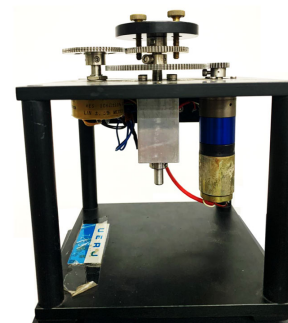**FIGURE 21.** Top view of the SRV-02 by Quanser.

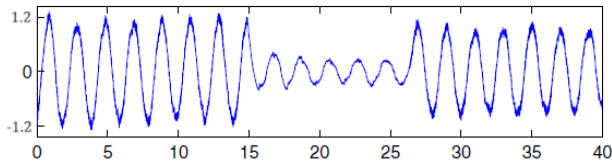**FIGURE 22.** DC motor (front view of the SRV-02 by Quanser).

FIGURE 23. Experiments using linear lead filter or nonlinear HOSM-based differentiator: output error z_1 (tracking a sinusoid). All angles expressed in degrees.
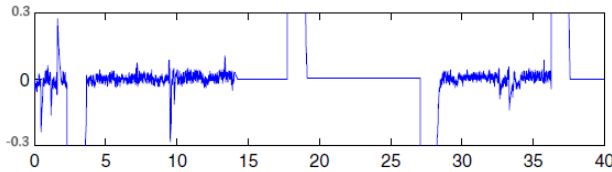

FIGURE 24. Experiments using linear lead filter or nonlinear HOSM-based differentiator: output error z_1 in response to step inputs. All angles expressed in degrees.
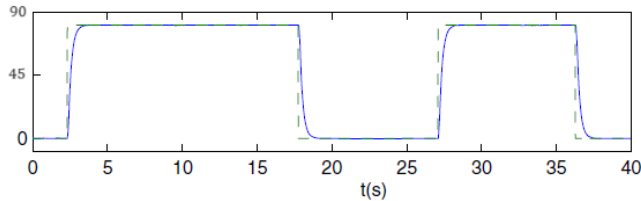

FIGURE 25. Experiments using linear lead filter or nonlinear HOSM-based differentiator: $y = x_1$ (solid) and reference step inputs (dashed). All angles expressed in degrees.

The aim of the experiment discussed here is to evaluate the practical advantage of using HOSM-based differentiators in adaptive backstepping control, compared to a linear lead filter, for a simple but real application, in order to obtain precise output tracking. In this experiment, the reference model (38) was chosen as $y_r(s) = \frac{20}{(s+5)(s+20)} r(s)$ and the linear lead filter given by (125), with $\tau_f = 2$ms. The HOSM-based differentiator is implemented as (114) and (115), with $\lambda_0 = 100$ and $\lambda_1 = 2500$.

In what follows, we discuss in detail the results of the experiment. In Figure 23, the linear lead filter is applied for $t \in [0, 16]$ seconds. Then, for $t \in [16, 26]$ seconds, it was manually switched to HOSM-based differentiator and, finally, it was switched back to the linear lead filter thereafter. One can clearly note the better performance of the nonlinear HOSM-based differentiator and the performance degradation caused by the phase lag of the linear lead filter, with $\tau_f = 2$ ms. This time constant was experimentally tuned as small as possible so that the control chattering was acceptable.

Figures 24 and 25 present the response of the system to step changes in the reference input $r(t)$. For $t \in [14, 28]$ seconds and $t \in [37, 40]$ seconds, only the nonlinear HOSM-based differentiator is used, while in the remaining intervals of

time, the linear lead filter is employed. Noticeable chattering results appear in the latter case, during the steady state in the step following experiment. In contrast, the chattering is practically eliminated in the case of the nonlinear HOSM-based differentiator. Thus, remarkably superior regulation performance is observed when the proposed method is used.

VIII. CONCLUSION

In this paper, a new *backstepping* adaptive controller was proposed for a class of nonlinear systems of the *strict-feedback* type. In addition, to simplify the original *back-stepping* adaptive controller, avoiding the use of partial derivatives in its control law, the use of the global *HOSM* differentiator with dynamic gains ensured a globally stable closed-loop control system. For any initial conditions, the control law will act leading to the convergence of the output to a desired trajectory.

According to the final numerical comparisons of distinct differentiation schemes being employed in the backstepping control law, we could conclude that the linear differentiators lead to a highly sensitive-adverse phenomenon of peaking. On the other hand, HOSM differentiators with fixed gains are valid only locally, demanding increments on the domain of attraction by increasing the constant gain of the differentiator. This results in a potential increase of the sensitivity of the overall closed-loop systems to real-world imperfections, such as noises and delays. Experimental results with a DC motor also support the advantages of obtaining a more precise output tracking with the proposed method.

For future works we could use the adaptive backstepping control for nonlinear systems to improve the research background, for example, event-based adaptive fixed-time fuzzy control for active vehicle suspension systems with time-varying displacement constraint [32], adaptive multi-gradient recursive reinforcement learning event-triggered tracking control for multiagent systems [33], nonsingular finite-time event-triggered fuzzy control for large-scale nonlinear systems [34]. We invite the readers to perform new experimental works on the topic for different engineering applications [35].

REFERENCES

[1] V. Utkin, "Variable structure systems with sliding modes," *IEEE Trans. Automat. Control*, vol. AC-22, no. 2, pp. 212–222, Apr. 1977.

[2] P. V. Kokotović, "The joy of feedback: Nonlinear and adaptive," *IEEE Control Syst. Mag.*, vol. 12, no. 3, pp. 7–17, Jun. 1992.

[3] M. Krstić, I. Kanellakopoulos, and P. V. Kokotović, *Nonlinear and Adaptive Control Design*. Hoboken, NJ, USA: Wiley, 1995.

[4] F. Zhu, Y. Zhao, Y. Fu, and T. N. Dinh, "Observer-based output consensus control scheme for strict-feedback nonlinear multi-agent systems with disturbances," *IEEE Trans. Netw. Sci. Eng.*, early access, Dec. 28, 2023, doi: 10.1109/TNSE.2023.3346442.

[5] L. Zhang, C. Deng, and L. An, "Asymptotic tracking control of nonlinear strict-feedback systems with state/output triggering: A homogeneous filtering approach," *IEEE Trans. Autom. Control*, early access, Mar. 29, 2024, doi: 10.1109/TAC.2024.3383090.

[6] S. A. Siffat, I. Ahmad, A. Ur Rahman, and Y. Islam, "Robust integral backstepping control for unified model of hybrid electric vehicles," *IEEE Access*, vol. 8, pp. 49038–49052, 2020, doi: 10.1109/ACCESS.2020.2978258.

[7] J. Fredriksson and B. Egardt, "Backstepping control with local LQ performance applied to a turbocharged diesel engine," in *Proc. IEEE 40th Conf. Decision Control*, Orlando, FL, USA, Dec. 2001, pp. 111–116.

[8] M. Krstic, D. Fontaine, and P. V. Kokotovic, "Useful nonlinearities and global stabilization of bifurcations in a model of jet engine surge and stall," *IEEE Trans. Automat. Control*, vol. 43, no. 12, pp. 1739–1745, Dec. 1998.

[9] Z. Xu, S. X. Yang, and S. A. Gadsden, "Enhanced bioinspired backstepping control for a mobile robot with unscented Kalman filter," *IEEE Access*, vol. 8, pp. 125899–125908, 2020, doi: 10.1109/ACCESS.2020.3007881.

[10] H. Nemati and A. Montazeri, "Output feedback sliding mode control of quadcopter using IMU navigation," in *Proc. IEEE Int. Conf. Mechatronics (ICM)*, vol. 1, Ilmenau, Germany, Mar. 2019, pp. 634–639, doi: 10.1109/ICMECH.2019.8722899.

[11] Q. Zhang and X. Zhang, "Nonlinear improved concise backstepping control of course keeping for ships," *IEEE Access*, vol. 7, pp. 19258–19265, 2019, doi: 10.1109/ACCESS.2019.2896146.

[12] J. S. Matthew, N. B. Knoebel, S. R. Osborne, R. W. Beard, and A. Eldredge, "Adaptive backstepping control for miniature air vehicles," in *Proc. Amer. Control Conf.*, 2006, p. 6, doi: 10.1109/acc.2006.1657678.

[13] J. A. Davila and G. C. G. Ez-Cortes, "Attitude control of spacecraft using robust backstepping controller based on high order sliding modes," in *Proc. AIAA*, Aug. 2013, p. 5121, doi: 10.2514/6.2013-5121.

[14] M. Krstic, I. Kanellakopoulos, and P. V. Kokotović, "Adaptive nonlinear control whithout overparametrization," *Syst. Control Lett.*, vol. 19, pp. 177–185, May 1992.

[15] D. Swaroop, J. K. Hedrick, P. P. Yip, and J. C. Gerdes, "Dynamic surface control for a class of nonlinear systems," *IEEE Trans. Autom. Control*, vol. 45, no. 10, pp. 1893–1899, Oct. 2000, doi: 10.1109/TAC.2000.880994.

[16] W. Dong, J. A. Farrell, M. M. Polycarpou, V. Djapic, and M. Sharma, "Command filtered adaptive backstepping," *IEEE Trans. Control Syst. Technol.*, vol. 20, no. 3, pp. 566–580, May 2012, doi: 10.1109/TCST.2011.2121907.

[17] J. Davila, "Exact tracking using backstepping control design and high-order sliding modes," *IEEE Trans. Autom. Control*, vol. 58, no. 8, pp. 2077–2081, Aug. 2013, doi: 10.1109/TAC.2013.2246894.

[18] K. Queiroz, S. Dias, A. Araújo, and D. Fernandes, "Simplificação de um controlador adaptativo backstepping para uma classe de sistemas não-lineares utilizando um diferenciador híbrido global," in *Proc. 11th Simpósio Brasileiro Automação Inteligente*, 2013, pp. 1–6.

[19] A. Levant, "Robust exact differentiation via sliding mode technique," *Automatica*, vol. 34, pp. 379–384, Aug. 1998.

[20] T. R. Oliveira, A. Estrada, and L. Fridman, "Global and exact HOSM differentiator with dynamic gains for output-feedback sliding mode control," *Automatica*, vol. 81, pp. 156–163, Jan. 2017.

[21] G. Kreisselmeier, "Adaptive observers with exponential rate of convergence," *IEEE Trans. Autom. Control*, vol. AC-22, no. 1, pp. 2–8, Feb. 1977.

[22] H. V. A. Truong, S. Nam, S. Kim, Y. Kim, and W. K. Chung, "Backstepping-sliding-mode-based neural network control for electro-hydraulic actuator subject to completely unknown system dynamics," *IEEE Trans. Autom. Sci. Eng.*, early access, Oct. 16, 2023, doi: 10.1109/TASE.2023.3323148.

[23] N. Xu, X. Liu, Y. Li, L. Zong, X. Zhao, and H. Wang, "Dynamic event-triggered control for a class of uncertain strict-feedback systems via an improved adaptive neural networks backstepping approach," *IEEE Trans. Autom. Sci. Eng.*, early access, Mar. 18, 2024, doi: 10.1109/TASE.2024.3374522.

[24] T. K. Nizami, "Design and implementation of online estimation based backstepping controller for DC–DC buck converters," Indian Inst. Technol. Guwahati, Guwahati, India, Tech. Rep. 10610229, 2017.

[25] T. R. Oliveira, A. Estrada, and L. M. Fridman, "Global exact differentiator based on higher-order sliding modes and dynamic gains for globally stable output-feedback control," in *Proc. 54th IEEE Conf. Decis. Control (CDC)*, Dec. 2015, pp. 4109–4114, doi: 10.1109/CDC.2015.7402859.

[26] V. H. P. Rodrigues and T. R. Oliveira, "Global adaptive HOSM differentiators via monitoring functions and hybrid state-norm observers for output feedback," *Int. J. Control*, vol. 91, no. 9, pp. 2060–2072, Sep. 2018, doi: 10.1080/00207179.2017.1392041.

[27] T. R. Oliveira, V. H. P. Rodrigues, and L. Fridman, "Generalized model reference adaptive control by means of global HOSM differentiators," *IEEE Trans. Autom. Control*, vol. 64, no. 5, pp. 2053–2060, May 2019.

[28] J. A. Moreno, "Exact differentiator with varying gains," *Int. J. Control*, vol. 91, no. 9, pp. 1983–1993, Sep. 2018.

[29] A. Levant and M. Livne, "Exact differentiation of signals with unbounded higher derivatives," *IEEE Trans. Autom. Control*, vol. 57, no. 4, pp. 1076–1080, Apr. 2012.

[30] M. Krstić, I. Kanellakopoulos, and P. V. Kokotović, "Nonlinear design of adaptive controllers for linear systems," *IEEE Trans. Autom. Control*, vol. 39, no. 4, pp. 752–783, Apr. 1994.

[31] A. N. Atassi and H. K. Khalil, "A separation principle for the stabilization of a class of nonlinear systems," in *Proc. Eur. Control Conf. (ECC)*, Jul. 1997, pp. 3829–3834.

[32] T. Jia, Y. Pan, H. Liang, and H.-K. Lam, "Event-based adaptive fixed-time fuzzy control for active vehicle suspension systems with time-varying displacement constraint," *IEEE Trans. Fuzzy Syst.*, vol. 30, no. 8, pp. 2813–2821, Aug. 2022, doi: 10.1109/TFUZZ.2021.3075490.

[33] H. Li, Y. Wu, M. Chen, and R. Lu, "Adaptive multigradient recursive reinforcement learning event-triggered tracking control for multiagent systems," *IEEE Trans. Neural Netw. Learn. Syst.*, vol. 34, no. 1, pp. 144–156, Jan. 2023, doi: 10.1109/TNNLS.2021.3090570.

[34] P. Du, Y. Pan, H. Li, and H.-K. Lam, "Nonsingular finite-time event-triggered fuzzy control for large-scale nonlinear systems," *IEEE Trans. Fuzzy Syst.*, vol. 29, no. 8, pp. 2088–2099, Aug. 2021, doi: 10.1109/TFUZZ.2020.2992632.

[35] T. R. Oliveira, L. Fridman, and L. Hsu, *Sliding-Mode Control and Variable-Structure Systems: The State of the Art*. Cham, Switzerland: Springer, 2023.

MARCELO LUIZ DE CARVALHO MOURA MOREIRA was born in Rio de Janeiro, Brazil, 1991. He received the B.Sc. and M.Sc. degrees in electrical engineering from the State University of Rio de Janeiro (UERJ), in 2016 and 2019, respectively. He is currently an Energy Research Analyst with the public Energy Research Office (EPE), working within the Department of Transmission Expansion Studies. He frequently carries out electrical engineering projects and studies for companies and individuals as a Freelancer. He recently worked in engineering coordination with the Federal University of the State of Rio de Janeiro (UNIRIO). He was a Professor of the electromechanics course with the Technical School Support Foundation (FAETEC), Helber Vignoli Muniz State Technical School (ETEHVM), and a Professor with Barra Mansa University Center (UBM) in the institution's electrical engineering course. He also worked with projects and maintenance in water and sewage treatment plants at Barra Mansa Autonomous Water and Sewage Service (SAAE-BM) and with management and supervision of works in distribution networks at ENEL-Rio. He has experience in installation projects, protection studies, and the electricity market. His current research interests include nonlinear control theory, extremum seeking, sliding mode control, and electrical systems planning and distribution networks.

TIAGO ROUX OLIVEIRA (Senior Member, IEEE) was born in Rio de Janeiro, Brazil, in 1981. He received the B.Sc. degree in electrical engineering from the State University of Rio de Janeiro (UERJ), in 2004, and the M.Sc. and Ph.D. degrees in electrical engineering from the Graduate School and Research in Engineering, Federal University of Rio de Janeiro (COPPE/UFRJ), in 2006 and 2010, respectively. In 2014, he was a Visiting Scholar with the University of California at San Diego (UCSD), San Diego, CA, USA. He is currently an Associate Professor with the Department of Electronics and Telecommunication Engineering (DETEL), UERJ. He published about 200 refereed journal articles, conference papers, and book chapters. He is the coauthor of the book entitled *Extremum Seeking Through Delays and PDEs* (SIAM), in 2022. His current research interests include nonlinear control theory, extremum seeking, sliding mode control/observers, time delays, and boundary control for partial differential equations. He has served as a member of the IFAC Technical Committees: Adaptive and Learning Systems (TC 1.2) and Control Design (TC 2.1), and the Technical Committee on Variable Structure and Sliding Mode Control of the IEEE Control Systems Society (CSS). In 2017, he was nominated as an Affiliate Member of the Brazilian Academy of Sciences (ABC). In 2018, he was elevated to the grade of a Senior Member of the IEEE CSS. He was a recipient of the Bolsa Nota 10 (Highest Rank Scholarship Prize) sponsored by the Brazilian Agency FAPERJ, the CAPES National Award of Best Thesis in Electrical Engineering, in 2011, and the FAPERJ Young Researcher Award, in 2012, 2015, and 2018. In 2021, he was awarded IEEE TRANSACTIONS ON CONTROL SYSTEMS TECHNOLOGY Outstanding Paper Award from the IEEE CSS. In 2020, he was elected and nominated as the Chair of the Technical Committee 1.2 (Adaptive and Learning Systems) of the IFAC, for the triennium 2020–2023, and thereafter reelected for the next triennium 2023–2026. He was the Guest Editor of the *International Journal of Adaptive Control and Signal Processing* in the Special Issue "From Adaptive Control to Variable Structure Systems - Seeking Harmony." He has served as an Associate Editor on the Editorial Board of *The Journal of the Franklin Institute*; *Journal of Control, Automation and Electrical Systems*; IEEE LATIN AMERICA TRANSACTIONS; *International Journal of Robust and Nonlinear Control*; *Systems and Control Letters*; IEEE OPEN JOURNAL OF CONTROL SYSTEMS; IEEE CONTROL SYSTEMS LETTERS; and *Automatica*. Since 2019, he has been an Associate Editor of the European Control Association Conference Editorial Board (EUCA-CEB). In 2023, he was elected as the President of the Brazilian Society of Automatics (SBA), for the biennium 2023–2025.

KURIOS IURI PINHEIRO DE MELO QUEIROZ received the M.S. and Ph.D. degrees in electrical engineering from the Federal University of Rio Grande do Norte (UFRN), Brazil, in 2008 and 2011, respectively. From 2007 to 2011, he was a Professor with the Federal Institute of Education, Science and Technology of Rio Grande do Norte (IFRN), Brazil. He is currently a Professor with the Department of Electrical Engineering, UFRN. His research interests include nonlinear systems, adaptive control, sliding mode control, and embedded systems.

● ● ●